

Response to Reviewer #1's comments on He et al. 2019 Atmospheric Physics and Chemistry manuscript

We thank the anonymous reviewer for thoroughly reading our manuscript and providing helpful comments and suggestions, which lead a significant improvement of our manuscript. The detailed responses to major point comments are listed below (text in *italic* and black is the reviewer's comments, and the normal text highlighted in blue is our response):

*The authors presented a study on ozone pollution trend and its sensitivity to key precursors in the US over 1990 – 2015. While the lack of measurement data of ozone precursors in time and space makes it difficult to study long-term trends in ozone chemistry, increasingly available model simulations may be in place for such analysis with caution exercised. This study represents such effort. Studies like this one are needed for information of changes in ozone chemistry due to climate change and anthropogenic emissions control. I have a few comments as follows.*

Response: We appreciate the positive comments from the anonymous reviewer, and the manuscript has been revised according to these comments as listed below.

\*Line numbers are based on the revised clean version of the manuscript.

*The authors stated that, to avoid introducing inconsistency for model evaluation caused by “direct comparison”, they used the EPA RSIG software to visualize the observed and modeled ozone values. The question I have is how they quantified the difference between the modeled and observed values besides directly comparing the modeled value from a grid and the observed value(s) contained in that grid. Incidentally, what did “gridded” mean in “AQS station data were gridded to the CMAQ grid” in the Figure 5 caption? Didn't they just superimpose the station data on the CMAQ simulated distribution there?*

Response: The direct comparison is usually conducted through sampling the grid of CMAQ where the AQS site is located. In our previous study (He et al., 2016), we found that due to the uneven distribution of AQS monitoring sites, the direct comparison of AQS observations and our 30-km CMAQ simulations could be of problem. Figure 1 adapted from He et al. (2016) presents the case study of the CMAQ evaluation over California. AQS monitoring sites are point measurements and usually concentrated in populous urban and suburban areas such as the Los Angeles basin where high ozone levels prevail, but sparse in rural areas where ozone concentrations are generally low. Therefore, sampling CMAQ grids over locations of these AQS sites could introduce important biases. At that time, we lacked the capability to process large amount of AQS observations to our modeling grid (i.e., regrid observations to model grids), so we only raised this question. Recently, EPA added the capability in the Remote Sensing Information Gateway (RSIG) system (<https://www.epa.gov/hesc/remote-sensing-information-gateway>), which can calculate the gridded values of air pollutants on a selected model grid. The RSIG software applied the inverse-distance-weighted method to calculate the gridded mean (<https://www.epa.gov/hesc/how-rsig-regrids-data>), which is not a simple arithmetic mean of AQS observations within the grid. To explain the problem of direct comparison and the unique characteristics and advantage of RSIG, we added the following sentence in Line 215 as “*The direct comparison is usually conducted through sampling the grid of CMAQ where the AQS site*

is located, while the distribution of AQS monitoring sites is usually uneven with more sites concentrated in populous urban and suburban areas where high ozone levels prevail. Sampling 30-km CMAQ grids over the locations of AQS measurements, i.e. direct comparison of averaged concentrations in the 900 km<sup>2</sup> CMAQ grid and pointwise AQS observations, could introduce important biases” and in Line 222 as “The RISG has the capability to ‘re-grid’ the AQS observations on a selected model grid using the inverse-distance-weighted method to calculate the gridded mean concentrations (<https://www.epa.gov/hesc/how-rsig-regrids-data>).”

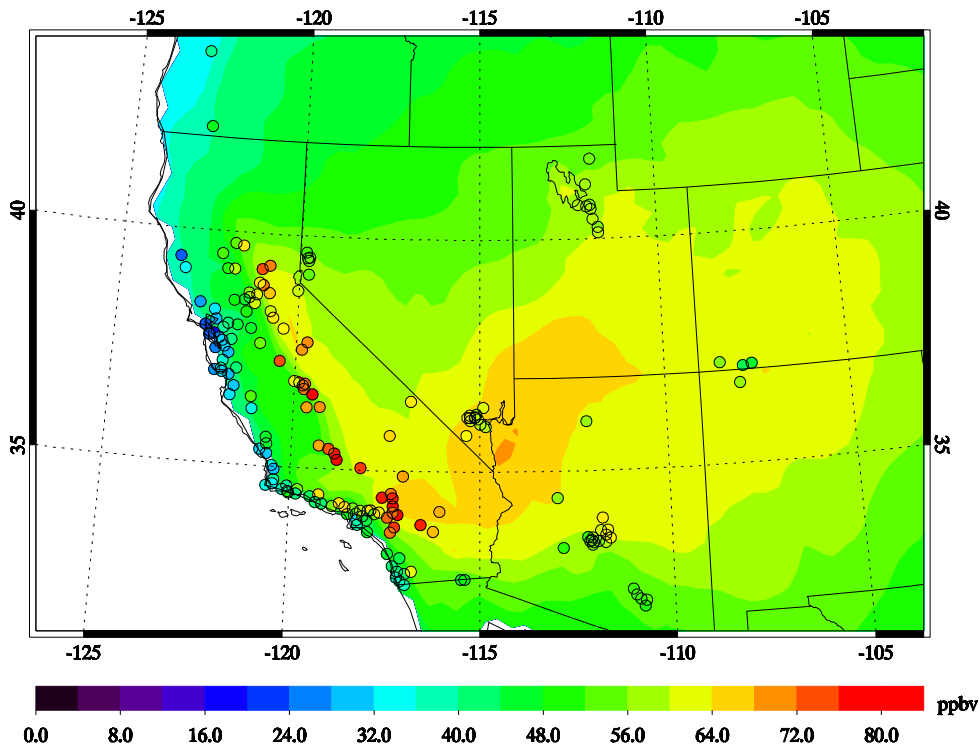


Figure 1. Comparison of EPA AQS ozone observations (color dots) and model simulations (background) in California (adapted from He et al. (2016)).

The authors stated that in subdomains CMAQ performance exhibited large interannual variations (Table 2) and they further stated that their CWRf-CMAQ simulations showed improved performance in the Northeast and Midwest. It would be illuminating to the modeling community if they could expand on those two statements by explaining why.

Response: We appreciate that the reviewer raised this question. Previous studies usually aggregate and average data from all modeling years into one analysis without considering interannual variations. Figure 2 shows a comparison using 2000-2015 data for the CONUS, which has better performance (NMB = -1.3%) than the year-by-year evaluation summarized in Table 2. In our manuscript, we conducted the evaluation by year for the CONUS and five subdomains, so we can identify the years with good and bad performance. With the assumption that our emissions reflect the gradual reduction of anthropogenic emissions in the past decades, the year-to-year fluctuations of model performance should be related to climate signals that control the regional ozone pollution. By doing so, we effectively reduced the impact of emissions reduction on the model performance. We are investigating the relationships between regional

climate characteristics and ozone pollution especially extreme pollution episodes, and hope to better address your question from the perspective of how extreme events affect interannual variations.

About the model improvement, we apologize that the current manuscript is not stated very clearly. These improvements were achieved through comparison with our previous study employing the CMM5-CMAQv4.7 modeling system (He et al. 2016). CMM5 is the previous generation of regional climate model, developed on the MM5 model. Our CWRf model has shown better performance for downscaling the U.S. climate and the updated CMAQ v5.2 has also improved. We have demonstrated that CWRf with more sophisticated physical processes (Liang et al., 2012) can simulate better regional climate variations in the United State including surface temperature and precipitation (Chen et al., 2016; Liu et al., 2016), especially for extreme events (Sun and Liang, 2020a; Sun and Liang, 2020b). These meteorological variables are key factors for better air quality simulations. To make these two points clear, we added following sentences and revised this paragraph in Line 233 as “*With gradual reduction in anthropogenic emissions, the fluctuations of CMAQ performance could be related to climate signals which control the regional ozone pollution. Future work is needed to identify the relationship between these regional climate variations and the U.S. ozone pollution*” and in Line 236 as “*Generally, this modeling system has substantially improved performance in the Southeast, California and Texas, and moderately improved performance in the Northeast and Midwest as compared with our previous modeling system (He et al., 2016), which significantly underestimated the U.S. ozone pollution. One reason is that CWRf with more sophisticated representation of physical processes have the capability to better simulate the U.S. climate especially surface temperature and precipitation (Liang et al., 2012; Chen et al., 2016; Liu et al., 2016; Sun and Liang, 2020b; Sun and Liang, 2020a), which are key to accurate air quality simulations. The evaluation of CMAQ performance demonstrates the capability of CWRf-CMAQ to credibly simulate historical air quality.*”

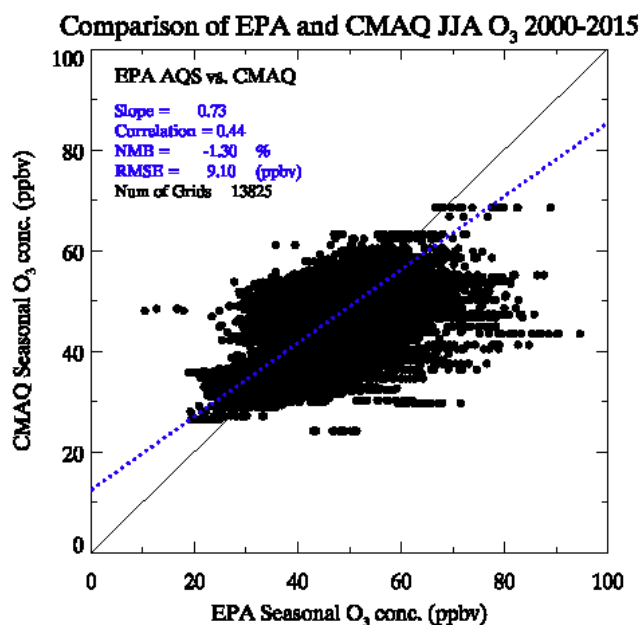


Figure 2. Similar as Figure 5b in the main article, but with data from 2000-2015

The authors brought up an interesting point that for Baltimore and Denver the peak ozone increased in some years after 2002 although anthropogenic emissions were continuously decreasing in the past decades. From there they inferred that the increased ozone pollution on those areas “could be caused by other factors such as higher summer temperatures in certain years or enhanced stratosphere-troposphere exchange” (lines 234-244). Their Figure 4 showed the largest peak of fires emissions over a couple of years starting in 2002, which could have influenced ozone during those years. Also, were the summer temperatures really higher and STE enhanced during those couple of years? The authors might want to avoid making such sheer speculations if they had no intention to get into making these points.

Response: Thanks for pointing out that the wildfire emissions could be an important source for the increasing summer ozone in some regions, especially Denver which could be impacted by the wildfire activities in the western United States. Another paper under review (Tao et al., *Remote Sensing*, 2020) confirmed the impacts from wildfires on air quality in the western United States. Another possibility is the change of ozone production regime, especially in Baltimore as discussed in the later section. We checked the temperature anomaly at Essex MD (AQS ID: 240053001, Fig. 3), which did not support our hypothesis. We agree that these speculations about possible high regional temperatures and STE lack evidences in current study, and removed these hypotheses in the revised manuscript.

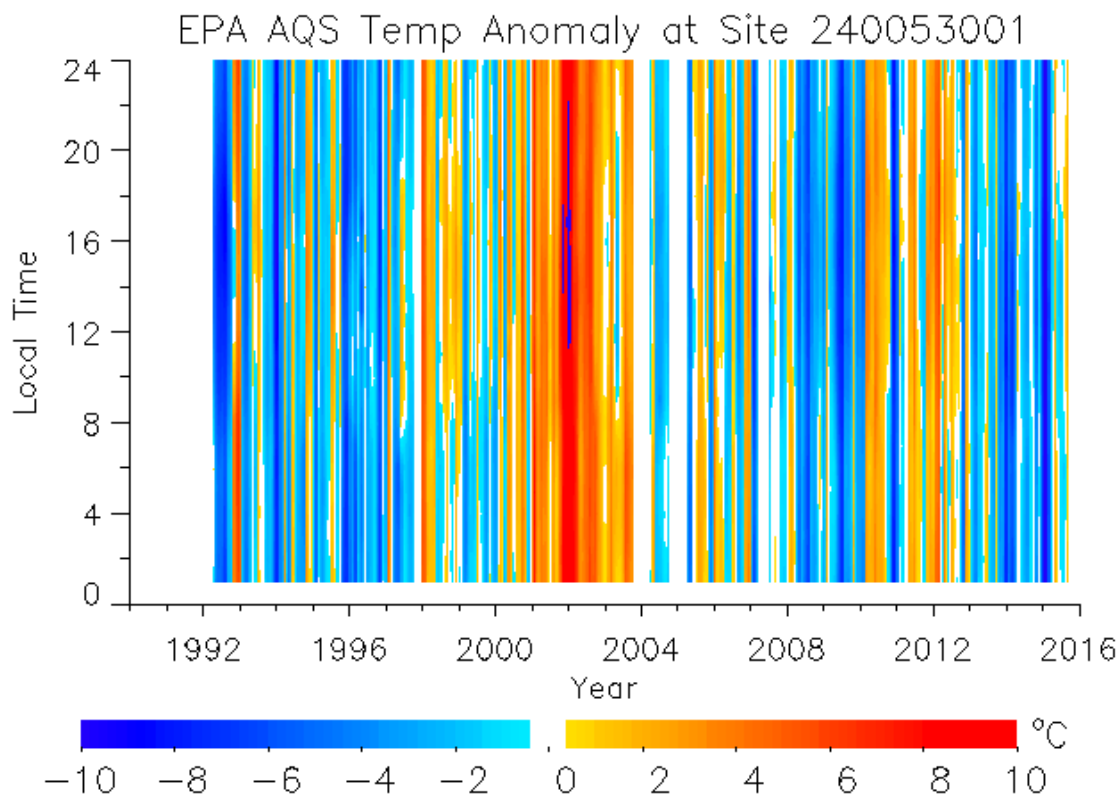


Figure 3. The AQS temperature anomaly at Essex, Maryland (Site ID: 240053001).

*I am a bit concerned with their threshold value of the O<sub>3</sub>/NO<sub>y</sub> ratio used to examine changes in the ozone formation regime. In our experience the model simulated O<sub>3</sub>/NO<sub>y</sub> ratio could differ greatly from the observed values and between simulations using different models. I am not sure if the threshold value of 15 from Zhang et al.(2009b), which used completely different models and had very different emissions and chemical environments, would be applicable. The authors need to find their own threshold value for their model simulations.*

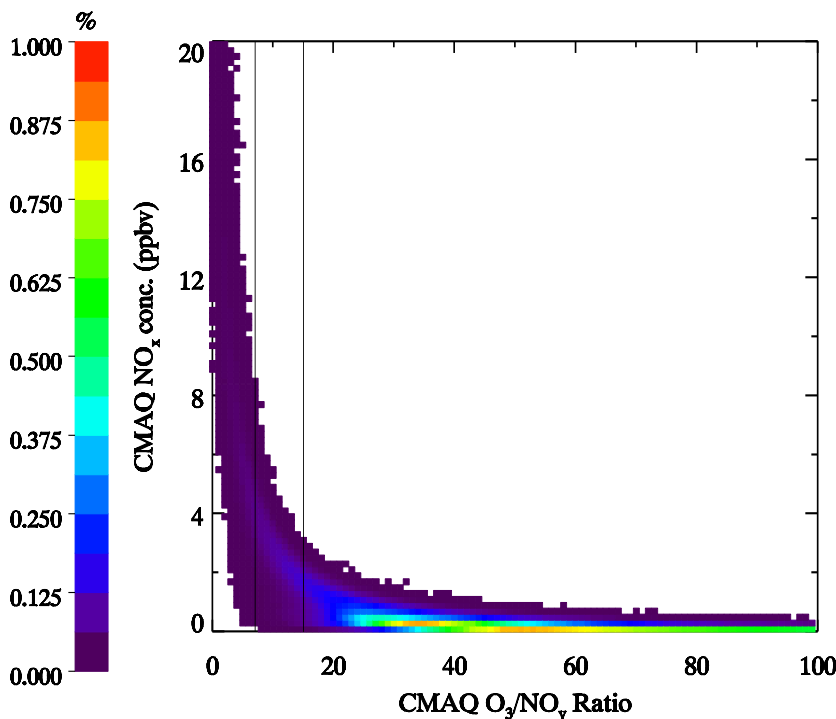
Response: Thanks for this important question. We understand that the model simulated O<sub>3</sub>/NO<sub>y</sub> ratio could differ largely from the observed values. In our study, we could not access the long record of research-grade NO<sub>y</sub> observations from the EPA network and did not conduct long-term sensitivity experiments of CMAQ with reduced emissions rates due to limited computation resources. So we have to rely on results from the previous studies. Sillman explored the concept using photochemical indicators including O<sub>3</sub>/NO<sub>y</sub> to identify the regime of ozone photochemical production, finding that the link between the ozone production sensitivity and these indicators is largely unaffected by changes in model assumptions, including emission rates of anthropogenic and biogenic species (Sillman, 1995; Sillman et al., 1997). Observations from urban areas of Atlanta, New York, and Los Angeles was compared with modeling results from the Urban Airshed Model at urban scales, and a threshold of 7 was proposed for using O<sub>3</sub>/NO<sub>y</sub> ratios as the photochemical indicator (Sillman et al., 1997). Zhang et al. (2009) expanded the study to the CONUS with 1-year CMAQ simulations, suggesting a threshold of 15 for O<sub>3</sub>/NO<sub>y</sub> ratios. Zhang et al. (2009) used previous CMAQ version 4.4 for 1-yr CONUS simulations of 2001 at a relatively coarse spatial resolution (36 km) which is close to our 30-km CONUS domain, so we adopted their proposed threshold. We agree that the current manuscript lacked the evaluation of this threshold with our modeling system, and we developed the following approach to test it.

We selected hourly O<sub>3</sub>, NO<sub>y</sub>, and NO<sub>x</sub> concentrations from CMAQ in the afternoon (defined as 12 pm to 4 pm) in 2014, and calculated the O<sub>3</sub>/NO<sub>y</sub> ratios. Figure 4a shows scatter density of O<sub>3</sub>/NO<sub>y</sub> ratios vs. NO<sub>x</sub> concentrations, which is calculated based on a 100 × 100 bins with NO<sub>x</sub> from 0-20 ppbv NO<sub>x</sub> (i.e., 0.2 ppbv per bin) and 0-100 O<sub>3</sub>/NO<sub>y</sub> ratios (i.e., 1 per bin). In the afternoon over the CONUS, the ozone production is mainly in high O<sub>3</sub>/NO<sub>y</sub> ratio (>15) and low NO<sub>x</sub> (less than 2 ppbv) environment, i.e., in the NO<sub>x</sub>-sensitive regions by thresholds proposed by both Sillman et al. (1997) and Zhang et al. (2009). Figure 4b shows the same density plot, but the color stands for mean O<sub>3</sub> concentrations. Both low and high ozone concentrations exist in high NO<sub>x</sub> region (NO<sub>x</sub> > 4 ppbv), which are usually urban or suburban. Then we calculated the weighted ozone concentrations that equals to the product of O<sub>3</sub>/NO<sub>y</sub> and NO<sub>x</sub> scatter density (Fig. 4a) and mean O<sub>3</sub> concentrations (Fig. 4b), which stands for the O<sub>3</sub> sensitivity with respect to O<sub>3</sub>/NO<sub>y</sub> ratios and NO<sub>y</sub> concentrations over the CONUS (Fig. 4c). At the national scale, when the weighted ozone concentrations increase with CMAQ NO<sub>x</sub> levels, the photochemical production is NO<sub>x</sub>-sensitive. The region with O<sub>3</sub>/NO<sub>y</sub> higher than 7 and 11 both have this characteristics, while due to low probability (Fig. 4a) and urban environment (Fig. 4b) we believe the O<sub>3</sub>/NO<sub>y</sub> threshold of 7 stands for the urban environment. Thus, the O<sub>3</sub>/NO<sub>y</sub> ratio threshold of 15 is more proper for the CONUS scale analysis. This analysis qualitatively supports our application of results from Zhang et al. (2009).

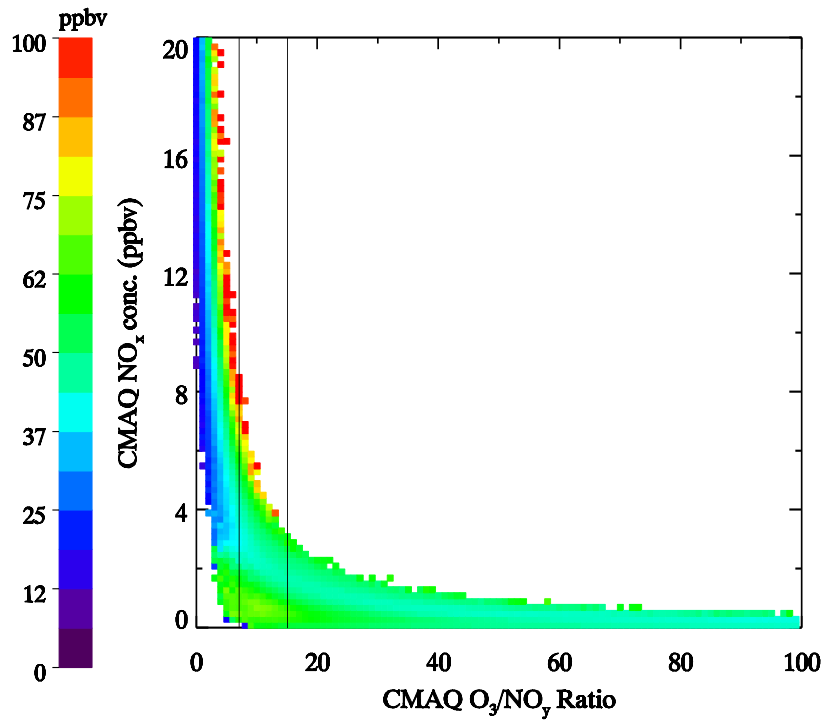
In summary, due to limited resources and experiment design, identifying a threshold of O<sub>3</sub>/NO<sub>y</sub> ratio is beyond the scope of this study. Using results from our CMAQ model, we proved that the threshold of 15 should be practical for our study. We added the following sentences in Line 323 as “*The usage of O<sub>3</sub>/NO<sub>y</sub> ratio was first proposed by Sillman (Sillman, 1995; Sillman et al.,*

1997). Sillman et al. (Sillman et al., 1997) conducted a case study of observations in urban areas (Atlanta, New York, and Los Angeles) and modeling results from the Urban Airshed Model and suggested the threshold of 7 as the transition region from VOC-sensitive environment to  $\text{NO}_x$ -sensitive environment. Zhang et al. (2009a; 2009b) expanded this method to the CONUS with 1-year observations and CMAQ simulations (36-km spatial resolution) and suggested a threshold of 15 for ozone pollution at the national scale. In this study, we did not have access to the long-term research grade  $\text{NO}_y$  observations from the AQS network and did not conduct sensitivity experiments (due to computational resource limit) with reduced  $\text{NO}_x$  emissions following Sillman et al. (1997), so we have to rely on the  $\text{O}_3/\text{NO}_y$  threshold from literature. We conducted a simple evaluation of our CMAQ results and found the threshold of 7 could be more proper for urban areas and the threshold of 15 should be more applicable for our study of the whole United State (Figure S1 in the supplementary material). Please note that the  $\text{O}_3/\text{NO}_y$  ratio could depend on the modeling framework, so due to the similarity of our modeling system (30-km CMAQ) and the model used in Zhang et al. (2009a; 2009b), our analysis suggests the similar threshold of 15” and the discussion above to the supplementary material.

a)



b)



c)

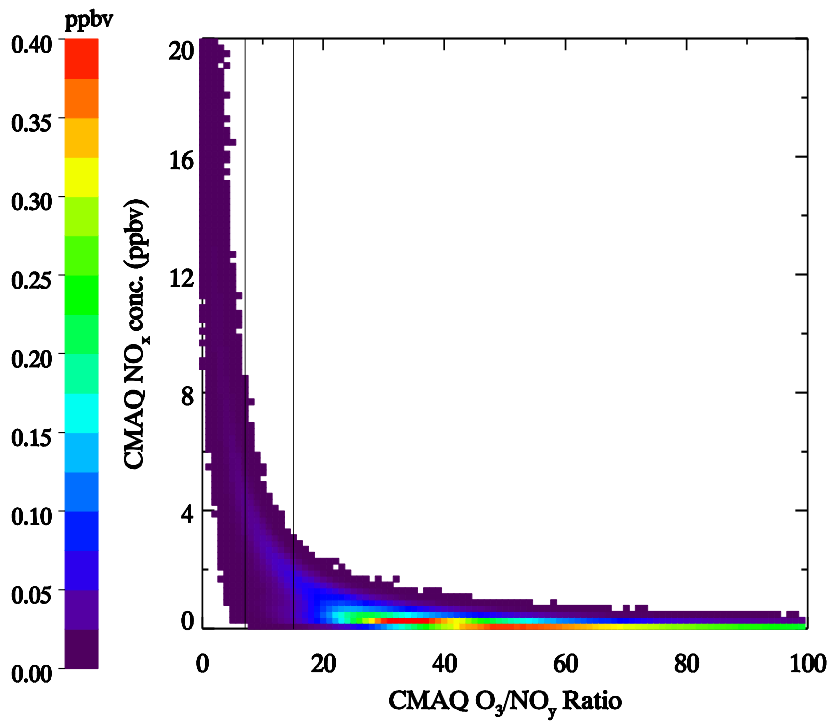


Figure 4. Afternoon O<sub>3</sub>/NO<sub>y</sub> ratios vs. NO<sub>x</sub> concentrations simulated by CMAQ in 2014. a) Scatter density, the color contour stands for the probability for each bin; b) O<sub>3</sub> concentrations, the color contour stands for the mean O<sub>3</sub> over the bins; c) Weighted O<sub>3</sub> concentrations. Two black lines stand for the O<sub>3</sub>/NO<sub>y</sub> ratios of 7 and 11.

Reference:

- Chen, L. G., Liang, X. Z., DeWitt, D., Samel, A. N., and Wang, J. X. L.: Simulation of seasonal US precipitation and temperature by the nested CWRP-ECHAM system, *Climate Dynamics*, 46, 879-896, 10.1007/s00382-015-2619-9, 2016.
- He, H., Liang, X.-Z., Lei, H., and Wuebbles, D. J.: Future U.S. ozone projections dependence on regional emissions, climate change, long-range transport and differences in modeling design, *Atmospheric Environment*, 128, 124-133, <https://doi.org/10.1016/j.atmosenv.2015.12.064>, 2016.
- Liang, X.-Z., Xu, M., Yuan, X., Ling, T., Choi, H. I., Zhang, F., Chen, L., Liu, S., Su, S., Qiao, F., He, Y., Wang, J. X. L., Kunkel, K. E., Gao, W., Joseph, E., Morris, V., Yu, T.-W., Dudhia, J., and Michalakes, J.: Regional Climate-Weather Research and Forecasting Model, *Bulletin of the American Meteorological Society*, 93, 1363-1387, 10.1175/bams-d-11-00180.1, 2012.
- Liu, S., Wang, J. X. L., Liang, X.-Z., and Morris, V.: A hybrid approach to improving the skills of seasonal climate outlook at the regional scale, *Climate Dynamics*, 46, 483-494, 10.1007/s00382-015-2594-1, 2016.
- Sillman, S.: The use of NO<sub>y</sub>, H<sub>2</sub>O<sub>2</sub>, and HNO<sub>3</sub> as indicators for ozone-NO<sub>x</sub>-hydrocarbon sensitivity in urban locations, *Journal of Geophysical Research-Atmospheres*, 100, 14175-14188, 10.1029/94jd02953, 1995.
- Sillman, S., He, D., Cardelino, C., and Imhoff, R. E.: The Use of Photochemical Indicators to Evaluate Ozone-NO<sub>x</sub>-Hydrocarbon Sensitivity: Case Studies from Atlanta, New York, and Los Angeles, *J. Air Waste Manage. Assoc.*, 47, 1030-1040, 10.1080/10962247.1997.11877500, 1997.
- Sun, C., and Liang, X. Z.: Improving U.S. extreme precipitation simulation: Sensitivity to physics parameterizations, *Climate Dynamics*, to be submitted, 2020a.
- Sun, C., and Liang, X. Z.: Improving U.S. extreme precipitation simulation: Dependence on cumulus parameterization and underlying mechanism, *Climate Dynamics*, to be submitted, 2020b.
- Zhang, Y., Wen, X. Y., Wang, K., Vijayaraghavan, K., and Jacobson, M. Z.: Probing into regional O<sub>3</sub> and particulate matter pollution in the United States: 2. An examination of formation mechanisms through a process analysis technique and sensitivity study, *Journal of Geophysical Research-Atmospheres*, 114, 10.1029/2009jd011900, 2009.



Response to Reviewer #3's comments on He et al. 2019 Atmospheric Physics and Chemistry manuscript

We thank the anonymous reviewer for thoroughly reading our manuscript and providing helpful comments and suggestions, which lead a significant improvement of our manuscript. The detailed responses to major point comments are listed below (text in *italic* and black is the reviewer's comments, and the normal text highlighted in blue is our response):

*This manuscript presents a modeling study of the decadal ozone trend in the US. I am impressed by the significance of the results, but there are still several important issues need to be addressed before publication.*

Response: We appreciate the positive comments from the anonymous reviewer, and the manuscript has been revised according to these comments as listed below.

\*Line numbers are based on the revised clean version of the manuscript.

*1 How will the results of CWRP-CMAQ differ from WRF-CMAQ? You can also use WRF to simulate decadal climate with long-term reanalysis. Better to include some description of the advantage of CWRP over WRF.*

Response: The CWRP was developed as a Climate extension of the WRF model incorporating numerous improvements in representation of physical processes and integration of external forcings that are crucial to climate scales, including interactions between land-atmosphere-ocean, convection-microphysics and cloud-aerosol-radiation, and system consistency throughout all process modules (Liang et al., 2012; Qiao and Liang, 2015; Chen et al., 2016; Liu et al., 2016; Qiao and Liang, 2016). It is built with a comprehensive ensemble of many alternate mainstream parameterization schemes for each of key physical processes. To better illustrate the advantage of CWRP, we added this short description in Line 127 of the revised manuscript.

*2 Scaling factors were used to get historical emissions. However, this will keep the spatial distribution the same at 2011 level. Why don't you use the information from other historical inventories, such as EDGAR? Could you discuss how this will affect the results?*

Response: This is a good question. The NEI2011 inventory adjusted with the ground and satellite measurements provides the best available anthropogenic emissions to the CONUS, which has also been used in the operational U.S. national air quality forecast. We used the U.S. National Emissions Trends to produce the scaling factors to generate historical emissions. It is not a perfect solution as pointed out by the reviewer that the assumption of the same spatial distribution may not be true. However, this method guaranteed that the domain total emissions would be consistent with the U.S. official emission trends, which we believe are the best available emissions for CONUS. We believe it is more important to provide total CONUS emissions constrained by the trend data than emissions with more detailed geographic distributions, when our modeling system has relatively coarse spatial resolution and integrates over 20 years. To explain our approach, we added the following sentences in Line 166 as "*Emissions of the baseline year are based on EPA NEI2011 inventory which can provide the best available anthropogenic emissions to the CONUS and are currently used in the operational U.S. national air quality forecast. The usage of APET scaling factors can guarantee the domain total emissions are consistent with the U.S. EPA emissions trend, although assuming the same spatial*

*distribution of anthropogenic emissions from year to year may not be realistic. Without a reasonable observation of actual spatiotemporal variations, it is the cost-effective approach as a first-order approximation to simulate long-term U.S. air quality driven by consistent CONUS total anthropogenic emissions that account interannual trends”.*

*3 Chemical initial and boundary conditions were obtained from the default concentration profiles built in CMAQ. For long lived chemical species like ozone, long range transport and stratospheric intrusions would be important. If default concentration profiles are set, how to consider the historical changes in sources outside the US?*

Response: We understand that the ICs and BCs are important to the CMAQ performance. To reduce the impacts of ICs, we spin-up the CMAQ model for two weeks before the 5-yr continuous simulations (e.g., two weeks in December 1999 were used to create ICs for 2000-2004 CMAQ simulations). Based on our experiences in CMAQ modeling and the EPA guidance, two weeks’ spin-up should be able to eliminate the influences from ICs.

The stratospheric intrusions are important for the ozone pollution in high altitude regions such as Denver, Colorado. However, the regional CMAQ does not include stratospheric chemistry, and our model top level is at 50 hPa. A potential vorticity (PV)-O<sub>3</sub> parameterization was developed recently for the hemispheric CMAQ model (Xing et al., 2016), but it is not available for the regional CMAQ version used in this study. We have discussed this shortcoming of our modeling system in the discussion section.

We agree that the long-range transport (LRT) through BCs can play an important role in the regional modeling of U.S. air quality. Our previous studies (He et al., 2016; He et al., 2018) show that the LRT can contribute up to 10% of ozone and PM<sub>2.5</sub> in the western United States; these numerical simulations are conducted in relatively short period (5 years) under multiple scenarios with fixed and dynamic LBCs. For climate studies, 5-year continuous integration is usually treated as the minimum time period, while longer simulation is preferred to better capture the climate signature. In this project, we designed a 25-yr experiment from 1990 to 2015, so CWRf downscaling can better represent the regional climate of the CONUS. Due to limited computing resources, we chose not conducting 25-yr global CTM simulations to generate dynamic LBCs conditions for CMAQ, but focused on the ozone pollution change within the United States. We understand that our approach could introduce some uncertainties in this study, and added the following sentences in Line 398 of the discussion session, “*So our current modeling system cannot take the historical changes of air pollution outside the United State into account. That is, the effect of long-range transport of air pollutants through model domain boundaries is presumed to be secondary to the long-term trends over the United States.*” and In Line 403 “*With these increased air pollutant transported into the United States, our study may underestimate the impacts of domestic emission reductions to U.S. ozone pollution, especially in the West Coast and the Southwest.*”.

*4 O<sub>3</sub>/NO<sub>y</sub> ratio was used as the indicator of VOC or NO<sub>x</sub> limited. The threshold of was adopted (O<sub>3</sub>/NO<sub>y</sub> < 15 indicating the VOC-sensitive regime). How to demonstrate this threshold and ratio is proper and accurate or represent the sensitivity. As model usually has difficulty in capturing the concentrations of NO<sub>y</sub>, the results might be questionable with this assumption.*

Response: We appreciate the reviewer raised this concern, which is also pointed out by the other reviewer. First, we understand that computer models have difficulty to accurately capture the

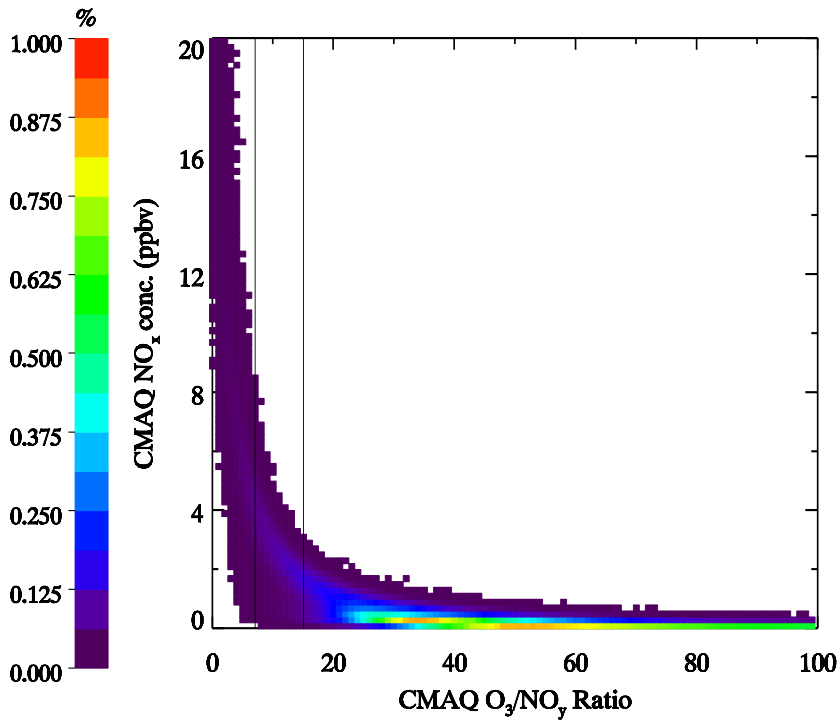
ambient  $\text{NO}_y$  concentrations. In this study, because we did not access long-term research grade  $\text{NO}_y$  observations from EPA, all the analysis using  $\text{O}_3/\text{NO}_y$  ratios as the photochemical indicators is based purely on CMAQ simulations. So we have to rely on results from the previous studies. Sillman explored the concept using photochemical indicators including  $\text{O}_3/\text{NO}_y$  to identify the regime of ozone photochemical production, finding that the link between the ozone production sensitivity and these indicators is largely unaffected by changes in model assumptions, including emission rates of anthropogenic and biogenic species (Sillman, 1995; Sillman et al., 1997). Observations from urban areas of Atlanta, New York, and Los Angeles was compared with modeling results from the Urban Airshed Model at urban scales, and a threshold of 7 was proposed for using  $\text{O}_3/\text{NO}_y$  ratios as the photochemical indicator (Sillman et al., 1997). Zhang et al. (2009) expanded the study to the CONUS with 1-year CMAQ simulations, suggesting a threshold of 15 for  $\text{O}_3/\text{NO}_y$  ratios. Zhang et al. (2009) used previous CMAQ version 4.4 for this 1-yr CONUS simulations of 2001 at a relatively coarse spatial resolution (36 km), which is close to our 30-km CONUS domain, so we adopted their proposed threshold. We agree that the current manuscript lacked the evaluation of this threshold with our modeling system, and we developed the following approach to test it.

We selected hourly  $\text{O}_3$ ,  $\text{NO}_y$ , and  $\text{NO}_x$  concentrations from CMAQ in the afternoon (defined as 12 pm to 4 pm) in 2014, and calculated the  $\text{O}_3/\text{NO}_y$  ratios. Figure 1a shows scatter density of  $\text{O}_3/\text{NO}_y$  ratios vs.  $\text{NO}_x$  concentrations, which is calculated based on a  $100 \times 100$  bins with  $\text{NO}_x$  from 0-20 ppbv  $\text{NO}_x$  (i.e., 0.2 ppbv per bin) and 0-100  $\text{O}_3/\text{NO}_y$  ratios (i.e., 1 per bin). In the afternoon over the CONUS, the ozone production is mainly in high  $\text{O}_3/\text{NO}_y$  ratio ( $>15$ ) and low  $\text{NO}_x$  (less than 2 ppbv) environment, i.e., in the  $\text{NO}_x$ -sensitive regions by thresholds proposed by both Sillman et al. (1997) and Zhang et al. (2009). Figure 1b shows the same density plot, but the color stands for mean  $\text{O}_3$  concentrations. Both low and high ozone concentrations exist in high  $\text{NO}_x$  region ( $\text{NO}_x > 4$  ppbv), which are usually urban or suburban. Then we calculated the weighted ozone concentrations that equals to the product of  $\text{O}_3/\text{NO}_y$  and  $\text{NO}_x$  scatter density (Fig. 1a) and mean  $\text{O}_3$  concentrations (Fig. 1b), which stands for the  $\text{O}_3$  sensitivity with respect to  $\text{O}_3/\text{NO}_y$  ratios and  $\text{NO}_y$  concentrations over the CONUS (Fig. 1c). At the national scale, when the weighted ozone concentrations increase with CMAQ  $\text{NO}_x$  levels, the photochemical production is  $\text{NO}_x$ -sensitive. The region with  $\text{O}_3/\text{NO}_y$  higher than 7 and 11 both have this characteristics, while due to low probability (Fig. 1a) and urban environment (Fig. 1b) we believe the  $\text{O}_3/\text{NO}_y$  threshold of 7 stands for the urban environment. Thus, the  $\text{O}_3/\text{NO}_y$  ratio threshold of 15 is more proper for the CONUS scale analysis. This analysis qualitatively supports our application of results from Zhang et al. (2009).

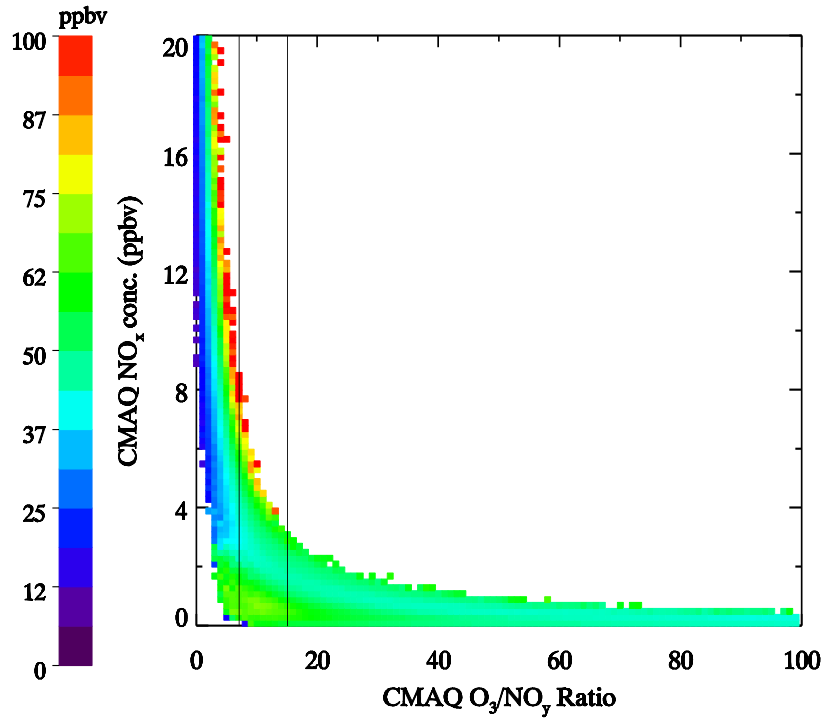
In summary, due to limited resources and experiment design, identifying a threshold of  $\text{O}_3/\text{NO}_y$  ratio is beyond the scope of this study. Using results from our CMAQ model, we proved that the threshold of 15 should be practical for our study. We added the following sentences in Line 323 as “*The usage of  $\text{O}_3/\text{NO}_y$  ratio was first proposed by Sillman (Sillman, 1995; Sillman et al., 1997). Sillman et al. (Sillman et al., 1997) conducted a case study of observations in urban areas (Atlanta, New York, and Los Angeles) and modeling results from the Urban Airshed Model and suggested the threshold of 7 as the transition region from VOC-sensitive environment to  $\text{NO}_x$ -sensitive environment. Zhang et al. (2009a; 2009b) expanded this method to the CONUS with 1-year observations and CMAQ simulations (36-km spatial resolution) and suggested a threshold of 15 for ozone pollution at the national scale. In this study, we did not have access to the long-term research grade  $\text{NO}_y$  observations from the AQS network and did not conduct sensitivity experiments (due to computational resource limit) with reduced  $\text{NO}_x$  emissions following Sillman*

*et al. (1997), so we have to reply on the  $O_3/NO_y$  threshold from literature. We conducted a simple evaluation of our CMAQ results and found the threshold of 7 could be more proper for urban areas and the threshold of 15 should be more applicable for our study of the whole United State (Figure S1 in the supplementary material). Please note that the  $O_3/NO_y$  ratio could depend on the modeling framework, so due to the similarity of our modeling system (30-km CMAQ) and the model used in Zhang et al. (2009a; 2009b), our analysis suggests the similar threshold of 15” and the discussion above to the supplementary material.*

a)



b)



c)

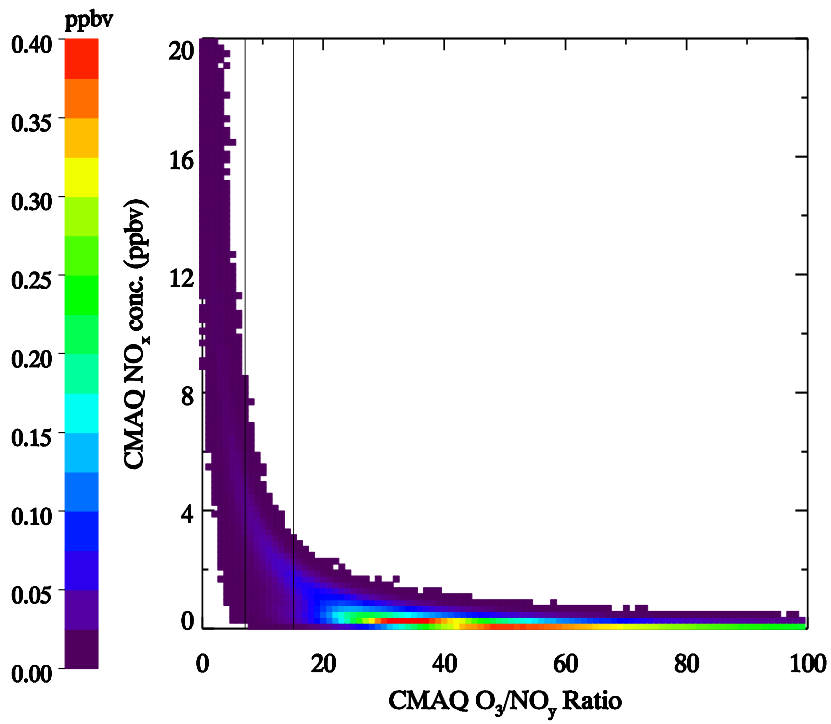


Figure 1. Afternoon O<sub>3</sub>/NO<sub>y</sub> ratios vs. NO<sub>x</sub> concentrations simulated by CMAQ in 2014. a) Scatter density, the color contour stands for the probability for each bin; b) O<sub>3</sub> concentrations, the color contour stands for the mean O<sub>3</sub> over the bins; c) Weighted O<sub>3</sub> concentrations. Two black lines stand for the O<sub>3</sub>/NO<sub>y</sub> ratios of 7 and 11.

#### Reference:

- Chen, L. G., Liang, X. Z., DeWitt, D., Samel, A. N., and Wang, J. X. L.: Simulation of seasonal US precipitation and temperature by the nested CWRP-ECHAM system, *Climate Dynamics*, 46, 879-896, 10.1007/s00382-015-2619-9, 2016.
- He, H., Liang, X.-Z., Lei, H., and Wuebbles, D. J.: Future U.S. ozone projections dependence on regional emissions, climate change, long-range transport and differences in modeling design, *Atmospheric Environment*, 128, 124-133, <https://doi.org/10.1016/j.atmosenv.2015.12.064>, 2016.
- He, H., Liang, X. Z., and Wuebbles, D. J.: Effects of emissions change, climate change and long-range transport on regional modeling of future US particulate matter pollution and speciation, *Atmospheric Environment*, 179, 166-176, 10.1016/j.atmosenv.2018.02.020, 2018.
- Liang, X.-Z., Xu, M., Yuan, X., Ling, T., Choi, H. I., Zhang, F., Chen, L., Liu, S., Su, S., Qiao, F., He, Y., Wang, J. X. L., Kunkel, K. E., Gao, W., Joseph, E., Morris, V., Yu, T.-W., Dudhia, J., and Michalakes, J.: Regional Climate-Weather Research and Forecasting Model, *Bulletin of the American Meteorological Society*, 93, 1363-1387, 10.1175/bams-d-11-00180.1, 2012.
- Liu, S., Wang, J. X. L., Liang, X.-Z., and Morris, V.: A hybrid approach to improving the skills of seasonal climate outlook at the regional scale, *Climate Dynamics*, 46, 483-494, 10.1007/s00382-015-2594-1, 2016.
- Qiao, F. X., and Liang, X. Z.: Effects of cumulus parameterizations on predictions of summer flood in the Central United States, *Climate Dynamics*, 45, 727-744, 10.1007/s00382-014-2301-7, 2015.
- Qiao, F. X., and Liang, X. Z.: Effects of cumulus parameterization closures on simulations of summer precipitation over the United States coastal oceans, *J. Adv. Model. Earth Syst.*, 8, 764-785, 10.1002/2015ms000621, 2016.
- Sillman, S.: The use of NO<sub>y</sub>, H<sub>2</sub>O<sub>2</sub>, and HNO<sub>3</sub> as indicators for ozone-NO<sub>x</sub>-hydrocarbon sensitivity in urban locations, *Journal of Geophysical Research-Atmospheres*, 100, 14175-14188, 10.1029/94jd02953, 1995.
- Sillman, S., He, D., Cardelino, C., and Imhoff, R. E.: The Use of Photochemical Indicators to Evaluate Ozone-NO<sub>x</sub>-Hydrocarbon Sensitivity: Case Studies from Atlanta, New York, and Los Angeles, *J. Air Waste Manage. Assoc.*, 47, 1030-1040, 10.1080/10962247.1997.11877500, 1997.
- Xing, J., Mathur, R., Pleim, J., Hogrefe, C., Wang, J., Gan, C. M., Sarwar, G., Wong, D. C., and McKeen, S.: Representing the effects of stratosphere-troposphere exchange on 3-D O<sub>3</sub> distributions in chemistry transport models using a potential vorticity-based parameterization, *Atmos. Chem. Phys.*, 16, 10865-10877, 10.5194/acp-16-10865-2016, 2016.

Zhang, Y., Wen, X. Y., Wang, K., Vijayaraghavan, K., and Jacobson, M. Z.: Probing into regional O<sub>3</sub> and particulate matter pollution in the United States: 2. An examination of formation mechanisms through a process analysis technique and sensitivity study, *Journal of Geophysical Research-Atmospheres*, 114, 10.1029/2009jd011900, 2009.

1 **The long-term trend and production sensitivity change of the U.S. ozone pollution from**  
2 **observations and model simulations**

3

4 Hao He<sup>1,2</sup>, Xin-Zhong Liang<sup>1,2</sup>, Chao Sun<sup>1</sup>, Zhining Tao<sup>3,4</sup>, and Daniel Q. Tong<sup>1,5</sup>

5 <sup>1</sup>Department of Atmospheric and Oceanic Science, University of Maryland, College Park,  
6 Maryland 20742, USA

7 <sup>2</sup>Earth System Science Interdisciplinary Center, University of Maryland, College Park, Maryland  
8 20740, USA

9 <sup>3</sup>Universities Space Research Association, Columbia, Maryland 21046, USA

10 <sup>4</sup>NASA Goddard Space Flight Center, Greenbelt, Maryland 20771, USA

11 <sup>5</sup>Center for Spatial Information Science and Systems, George Mason University, Fairfax, VA  
12 22030, USA

13

14 **Keywords:** Air Quality Trend, CMAQ Simulations, Ozone Production Sensitivity

15

16 Corresponding to Dr. Xin-Zhong Liang ([xliang@umd.edu](mailto:xliang@umd.edu))

17



18 **Abstract**

19 We investigated the ozone pollution trend and its sensitivity to key precursors from 1990  
20 to 2015 in the United States using long-term EPA AQS observations and mesoscale simulations.  
21 The modeling system, a coupled regional climate – air quality (CWRP-CMAQ) model, well  
22 captured summer surface ozone pollution during the past decades, having a mean slope of linear  
23 regression with AQS observations at ~0.75. While the AQS network has limited spatial coverage  
24 and measures only a few key chemical species, the CWRP-CMAQ provides comprehensive  
25 simulations to enable a more rigorous study of the change in ozone pollution and chemical  
26 sensitivity. Analysis of seasonal variations and diurnal cycle of ozone observations showed that  
27 peak ozone concentrations in the summer afternoon decreased ubiquitously across the United  
28 States, up to 0.5 ppbv/yr in major non-attainment areas such as Los Angeles, while  
29 concentrations at other hours such as the early morning and late afternoon increased slightly.  
30 Consistent with the AQS observations, CMAQ simulated a similar decreasing trend of peak  
31 ozone concentrations in the afternoon, up to 0.4 ppbv/yr, and increasing ozone trends in the early  
32 morning and late afternoon. ~~While a~~ monotonic decreasing trend (up to 0.5 ppbv/yr) in the odd  
33 oxygen ( $O_x = O_3 + NO_2$ ) concentrations are simulated by CMAQ at all daytime hours. This result  
34 suggests that the increased ozone in the early morning and late afternoon was likely caused by  
35 reduced NO-O<sub>3</sub> titration driven by continuous anthropogenic NO<sub>x</sub> emission reductions in the past  
36 decades. Furthermore, the CMAQ simulations revealed a shift in chemical regimes of ozone  
37 photochemical production. From 1990 to 2015, surface ozone production in some metropolitan  
38 areas, such as Baltimore, has transited from VOC-sensitive environment (>50% probability) to  
39 NO<sub>x</sub>-sensitive regime. Our results demonstrated that the long-term CWRP-CMAQ simulations  
40 can provide detailed information of the ozone chemistry evolution under a changing climate, and

41 may partially explain the U.S. ozone pollution responses to regional and national regulations.

42

## 43 **1. Introduction**

44 Tropospheric ozone ( $O_3$ ) is one of the major air pollutants, regulated by the U.S.  
45 Environmental Protection Agency (EPA), that pose myriad threats to public health and the  
46 environment (Adams et al., 1989; WHO, 2003; Ashmore, 2005; Anderson, 2009; Jerrett et al.,  
47 2009). It is also an important greenhouse gas due to the absorption of thermal radiation, affecting  
48 the climate (Fishman et al., 1979; Ramanathan and Dickinson, 1979; IPCC, 2013). The major  
49 source of tropospheric ozone is photochemical production from ozone precursors such as carbon  
50 monoxide (CO), volatile organic compounds (VOCs), and nitrogen oxides ( $NO_x$ ) at the presence  
51 of sunlight (Crutzen, 1974; Seinfeld, 1991; Jacob, 2000; EPA, 2006), while downward transport  
52 of stratospheric air mass contributes substantially to ozone concentrations in upper troposphere  
53 (Levy et al., 1985; Holton et al., 1995; Stevenson et al., 2006). In the past decades, ozone  
54 pollution in the United States has been reduced substantially due to regulations on anthropogenic  
55 emissions of ozone precursors (Oltmans et al., 2006; Lefohn et al., 2008, 2010; Cooper et al.,  
56 2012; He et al., 2013; Cooper et al., 2014), although some studies suggested no trend or slight  
57 increases at some rural areas (Jaffe and Ray, 2007; Lefohn et al., 2010; Cooper et al., 2012).  
58 Most of these analyses focused on peak ozone concentrations, e.g., daily maximum 8-hour  
59 average ozone (MDA8), during summer, but studies on trends in seasonal and diurnal patterns of  
60 ozone pollution are limited. He et al. (2019) analyzed measurements from four monitoring sites  
61 in the eastern United States and found different ozone trends between rural and urban sites from  
62 the late 1990s to the early 2010s including some increases at certain hours, suggesting effects of  
63 national regulations could be regionally dependent. Thus, it is important to extend our study to

64 other regions of the United States in a longer time period.

65         The non-monotonic trends in United States ozone pollution could be caused by the  
66 complex non-linear chemistry of ozone production involving  $\text{NO}_x$  and VOCs (Logan et al., 1981;  
67 Finlayson-Pitts and Pitts, 1999; Seinfeld and Pandis, 2006). With continuous reduction of  
68 anthropogenic emissions of ozone precursors mainly  $\text{NO}_x$  and VOCs in the United States, we  
69 need to better understand the photochemical regime change for local ozone production (i.e.,  
70 ozone production sensitivity), because air pollution regulations could have different effects under  
71  $\text{NO}_x$ -sensitive and VOC-sensitive environment (Dodge, 1987; Kleinman, 1994). For instance,  
72 under a VOC-sensitive photochemical regime, the decrease of  $\text{NO}_x$  emissions has limited  
73 impacts on improving ozone pollution. Previous studies have developed photochemical  
74 indicators to identify the ozone production sensitivity (Sillman, 1995; Sillman et al., 1997;  
75 Tonnesen and Dennis, 2000b, 2000a; Sillman and He, 2002). Sillman (1999) found the ratio of  
76 VOCs and  $\text{NO}_x$  ( $\text{VOC}/\text{NO}_x$ ) has a typical value less than 4 for the VOC-sensitive environment  
77 and higher than 15 for the  $\text{NO}_x$ -sensitive regime. Observation-based studies of ozone production  
78 sensitivity relied on research grade measurements of ozone precursors and photochemical  
79 intermediates that are not routinely measured by air quality management agencies such as the  
80 U.S. EPA. These species include reactive nitrogen compounds ( $\text{NO}_y$ ), nitric acid ( $\text{HNO}_3$ ), and  
81 hydrogen peroxide ( $\text{H}_2\text{O}_2$ ), normally observed during field campaigns (e.g., Shon et al., 2007;  
82 Peng et al., 2011) which only covered limited areas in certain periods. Studies based on air  
83 quality models (AQM) could identify the ozone production regimes at regional scales (Sillman et  
84 al., 1997; Sillman and He, 2002; Zhang et al., 2009a; Zhang et al., 2009b; Xie et al., 2011), but  
85 the simulation periods were usually short (less than one year) and thus could not capture the  
86 long-term change in ozone production sensitivity.

87 Regional AQMs are widely used for investigating the U.S. air quality (Tagaris et al.,  
88 2007; Tang et al., 2009; Hogrefe et al., 2011; Pour-Biazar et al., 2011; He et al., 2016a; He et al.,  
89 2018). They incorporate finer resolutions, more detailed emissions, and more explicit chemical  
90 mechanism than global chemical transport models to better resolve characteristics of  
91 tropospheric and surface dynamics, physical and chemical processes essential for air quality. Our  
92 group has developed and used coupled regional climate-air quality models to study air quality  
93 variations under a changing regional climate (Huang et al., 2007; Zhu and Liang, 2013; He et al.,  
94 2016a; He et al., 2018). Our previous studies showed the model's ability to capture the decadal  
95 U.S. air quality change (e.g., Zhu and Liang, 2013). In this study, we coupled the latest Climate-  
96 Weather Research Forecast (CWRF) and the EPA Community Multiscale Air Quality (CMAQ)  
97 models. CWRF has demonstrated substantial improvement in downscaling regional climate and  
98 extremes (Liang et al., 2012; Chen et al., 2016; Liu et al., 2016; Liang et al., 2019; Sun and  
99 Liang, 2020a; Sun and Liang, 2020b) and thus can provide more realistic weather conditions for  
100 AQMs to produce more credible air quality simulations.

101 To supplement the limited observations in both spatial coverage and chemical species, we  
102 conducted a continuous 26-yr CWRF-CMAQ simulation from 1990 to 2015 for a more rigorous  
103 analysis of long-term U.S. ozone trend. The model performance of the U.S. air quality was first  
104 evaluated against gridded ozone observations. The ozone seasonal variations and diurnal cycles  
105 were then extracted to determine the observed long-term trend. The model simulations were  
106 subsequently analyzed to explain the observed ozone trends and change in ozone production  
107 sensitivity.

## 108 2. Observations and model simulations

### 109 2.1 Long-term EPA observations

110 Hourly measurements of surface ozone concentrations from 1990 to 2015 were available  
111 from the EPA Air Quality System (AQS) database ([https://www.epa.gov/outdoor-air-quality-](https://www.epa.gov/outdoor-air-quality-data)  
112 [data](https://www.epa.gov/outdoor-air-quality-data)). They have been examined following the EPA guidance including the quality assurance and  
113 quality control. The locations and durations of AQS monitoring sites have changed substantially  
114 due to logistics and requirements to cover the regions sensitive to air pollution. Figure 1 shows  
115 that more than 2000 sites which reported ozone measurements ~~from~~ during the period of 1990 to  
116 2015. To alleviate the impacts from missing data and short durations, we selected 640 sites that  
117 had ozone observation records longer than 20 years. Hourly ozone observations were processed  
118 following the approach described in He et al. (2019) to create the long-term seasonal and diurnal  
119 records for these stations.

120

### 121 2.2 Regional climate modeling

122 CWRF (Liang et al., 2012) was driven by the European Centre for Medium-Range  
123 Weather Forecasts ERA-Interim reanalysis (ERI, Dee et al., 2011) to downscale regional climate  
124 variations during 1989-2015 with the first year as the spin-up and not used. We adopted the well-  
125 established CWRF North American domain with a 30-km grid spacing (Fig. 1), covering the  
126 Contiguous United States (CONUS) and neighboring southern Canada, northern Mexico and  
127 adjacent oceans. The CWRF was developed as a climate extension of the WRF model  
128 (Skamarock et al., 2008) incorporating numerous improvements in representation of physical  
129 processes and integration of external forcings that are crucial to climate scales, including  
130 interactions between land-atmosphere-ocean, convection-microphysics and cloud-aerosol-

131 ~~radiation, and system consistency throughout all process modules~~ (Liang et al., 2012; Qiao and  
132 Liang, 2015; Chen et al., 2016; Liu et al., 2016; Qiao and Liang, 2016). ~~CWRF is built with a~~  
133 ~~comprehensive ensemble of many alternate mainstream parameterization schemes for each of~~  
134 ~~key physical processes. The CWRF incorporated advanced representations of key physical~~  
135 ~~processes and integrations of external forcings crucial to climate scales (Liang et al., 2012).~~ It  
136 has been vigorously tested in North America and Asia showing outstanding performance to  
137 capture regional climate characteristics (Yuan and Liang, 2011; Chen et al., 2016; Liu et al.,  
138 2016; Liang et al., 2019). The CWRF downscaling has been shown to provide realistic  
139 meteorological fields and regional climate signals that can be cordially used to drive the CMAQ  
140 for long air quality simulations. Major CWRF physics configurations include the semi-empirical  
141 cloudiness parameterization of Xu and Randall (1996), the cloud microphysics scheme of Tao et  
142 al. (1989), the short wave and long wave radiation scheme of Chou et al. (2001), the ensemble  
143 cumulus parameterization (Qiao and Liang, 2015, 2016; Qiao and Liang, 2017), and the  
144 planetary boundary layer scheme of Holtslag and Boville (1993). Hourly CWRF outputs were  
145 processed using a modified Meteorology-Chemistry Interface Processor (MCIP, version 4.3) for  
146 CMAQ simulations.

147

### 148 **2.3 Emissions preparation**

149 To prepare anthropogenic emissions, we chose 2014 as the baseline year. This year's  
150 emissions were modified from the National Emissions Inventory 2011 (NEI2011). The  
151 modifications were based on measurements from the Ozone Monitoring Instrument (OMI)  
152 onboard satellite Aura, the ground-based AQS network, and the *in-situ* continuous emissions  
153 monitoring in power plants (Tong et al., 2015; Tong et al., 2016). The so modified NEI2011

154 inventory was processed using the Sparse Matrix Operator Kernel Emissions (SMOKE) version  
155 3.7 (Houyoux et al., 2000). Emissions from on-road, off-road, and area sources were placed at  
156 the model layer closest to the surface. Emissions from point sources, e.g., stacks from power  
157 plants, were distributed vertically based on stack height and plume rise. The plume rise was  
158 estimated based on the method in Briggs (1972). The inventory pollutants were speciated  
159 according to the carbon bond chemical mechanism version 5 (CB05) and AERO5 aerosol  
160 mechanism. To fill the gap where NEI2011 data were not available, the Emissions Database for  
161 Global Atmospheric Research (EDGAR v3, <http://edgar.jrc.ec.europa.eu/>) at a  $1^\circ \times 1^\circ$  resolution  
162 developed by the Joint Research Centre of European Commission was adapted. Figure 2 shows  
163 an example of 2010-2015 mean  $\text{NO}_x$  emissions distribution over the modeling domain. Daily  
164 mean  $\text{NO}_x$  emissions have high values in urban areas of cities such as Los Angeles, Chicago, and  
165 the northeast corridor from Washington D.C. to Boston.

166 To project emissions from the baseline year into all individual years, we used the scaling  
167 factors from Air Pollutant Emissions Trends (~~APET~~ ~~Data~~ ~~data~~) compiled by the U.S. EPA  
168 (<https://www.epa.gov/air-emissions-inventories/air-pollutant-emissions-trends-data>). Emissions  
169 of the baseline year are based on EPA NEI2011 inventory which can provide the best available  
170 anthropogenic emissions to the CONUS and are currently used in the operational U.S. national  
171 air quality forecast. The usage of APET scaling factors can guarantee the domain total emissions  
172 are consistent with the U.S. EPA emissions trend, although assuming the same spatial  
173 distribution of anthropogenic emissions from year to year may not be realistic. Without a  
174 reasonable observation of actual spatiotemporal variations, it is the cost-effective approach as a  
175 first-order approximation to simulate long-term U.S. air quality driven by consistent CONUS  
176 total anthropogenic emissions that account interannual trends. Figure 3 shows the emission

177 evolution from 1990 to 2015. Since 1990 anthropogenic emissions of NO<sub>x</sub>, CO, sulfur dioxide  
178 (SO<sub>2</sub>), and VOCs had steady decreasing trends, with SO<sub>2</sub> experiencing the largest reduction. On  
179 the other hand, anthropogenic PM<sub>2.5</sub> and NH<sub>3</sub> emissions stayed mostly flat since the early 2000s.

180 The wildfire emissions were based on the Global Fire Emissions Database, Version 4 with  
181 small fires (GFEDv4s, Randerson et al., 2017; van der Werf et al., 2017). The 0.25° × 0.25°  
182 degree resolution GFEDv4s data were projected onto the modeling domain and speciated into the  
183 CB05 and AERO5 species. GFEDv4s had a monthly resolution from 1997 to 2000 and daily  
184 resolution from 2000 onward. Figure 4 illustrates the fire emissions evolution during 1990 to  
185 2015 relative to 2014. Fire emissions have large interannual variations, with high emissions in  
186 1998, 2002, 2013, and 2015, and low emissions in 2001, 2004, and 2014. We developed a  
187 method to merge the aforementioned anthropogenic and wildfire emissions into the  
188 temporalized, gridded and speciated data ready for CMAQ.

189 | The biogenic emissions were calculated on-line within CMAQ based on the Biogenic  
190 Emissions Landuse Database, Version 3 (BELD3, [https://www.epa.gov/air-emissions-](https://www.epa.gov/air-emissions-modeling/biogenic-emissions-landuse-database-version-3-beld3)  
191 [modeling/biogenic-emissions-landuse-database-version-3-beld3](https://www.epa.gov/air-emissions-modeling/biogenic-emissions-landuse-database-version-3-beld3)). The 1-km resolution BELD3  
192 data with spatial distribution of 230 vegetation classes over the North America were processed  
193 through the Spatial Allocator developed by the Community Modeling and Analysis System  
194 (CMAS) center (<https://www.cmascenter.org/sa-tools/>) to generate the gridded vegetation  
195 distribution over the study domain. Table 1 lists the 5-yr mean variations of daily major ozone  
196 precursor (CO, NO<sub>x</sub>, and NMVOCs) emissions in the modeling domain and five subdomains.  
197 The emission data show regionally dependent reductions. For instance, compared with 2000-  
198 2004, the NO<sub>x</sub> emissions in 2005-2009 decreased by ~36% averaged in the CONUS, while 38%  
199 and 35% reductions existed in states of California and Texas.



## 200 **2.4 Air quality modeling**

201           The EPA CMAQ model version 5.2 (EPA, 2017) was selected to simulate the U.S. air  
202 quality variations driven by CWRM meteorological fields (Section 2.2) and constructed emissions  
203 (Section 2.3). Major chemical mechanisms include the Carbon Bond 6 revision 3 (CB6r3) gas  
204 phase chemical scheme with updated secondary organic aerosol (SOA) and nitrate chemistry  
205 (Yarwood et al., 2010) and the latest AERO6 aerosol scheme (EPA, 2017), which improved U.S.  
206 air quality simulations over previous chemical mechanisms (Appel et al., 2016). Chemical initial  
207 and boundary conditions were obtained from the default concentration profiles built in CMAQ  
208 (EPA, 2017). Simulations were conducted continuously for each 5-year segment (e.g., 1990-  
209 1994, 1995-1999, etc.) with two-week spin-up in December prior to each starting years to speed  
210 up simulation turn around. Hourly concentrations of ozone and its key precursors such as nitric  
211 | oxide (NO) and nitrogen dioxide (NO<sub>2</sub>) were saved for subsequent analyses.

212

## 213 **3. Results**

### 214 **3.1 Evaluation of CMAQ performance**

215           Our previous studies showed that the direct comparison of observation data from  
216 monitoring sites and CMAQ results in 30-km grid could introduce inconsistency for evaluating  
217 | the model performance (He et al., 2016a). The direct comparison is usually conducted through  
218 sampling the grid of CMAQ where the AQS site is located, while the distribution of AQS  
219 monitoring sites is usually uneven with more sites concentrated in populous urban and suburban  
220 areas where high ozone levels prevail. Sampling 30-km CMAQ grids over the locations of AQS  
221 measurements, i.e. direct comparison of averaged concentrations in the 900 km<sup>2</sup> CMAQ grid and  
222 pointwise AQS observations, could introduce important biases. So we applied the EPA Remote

223 Sensing Information Gateway (RSIG) software (available at <https://www.epa.gov/rsig>) to map  
224 the site observations onto our CMAQ grid. The RISG has the capability to ‘re-grid’ the AQS  
225 observations on a selected model grid using the inverse-distance-weighted method to calculate  
226 the gridded mean concentrations (<https://www.epa.gov/hesc/how-rsig-regrids-data>). Figure 5  
227 compares summer (JJA) mean MDA8 ozone in 2014 between gridded AQS observations and  
228 CMAQ outputs and shows that the model can well capture the U.S. ozone pollution, except  
229 underestimation in urban areas such as the Los Angeles basin.

230 Table 2 summarized the statistics ~~for~~of CMAQ performance ~~of~~simulating the summer  
231 ozone concentrations during 2000 - 2015 in CONUS and subdomains. Linear regression analyses  
232 of MDA8 ozone result in a mean slope value of 0.75 for CONUS, i.e., CMAQ slightly  
233 underestimates ozone over the United States. In subdomains, CMAQ performance exhibits large  
234 interannual variations. For instance, in Texas the linear regression slope and correlation  
235 coefficient ranges from 0.58 to 0.97 and 0.55 to 0.86, respectively. With gradual reduction in  
236 anthropogenic emissions, the fluctuations of CMAQ performance could be related to climate  
237 signals which control the regional ozone pollution. Future work is needed to identify the  
238 relationship between these regional climate variations and the U.S. ozone pollution. Generally,  
239 this modeling system has substantially improved performance in the Southeast, California and  
240 Texas, and moderately improved performance in the Northeast and Midwest as compared with  
241 our previous ~~study modeling system~~ (He et al., 2016a), which significantly underestimated the  
242 U.S. ozone pollution. One reason is that CWRF with more sophisticated representation of  
243 physical processes have the capability to better simulate the U.S. climate especially surface  
244 temperature and precipitation (Liang et al., 2012; Chen et al., 2016; Liu et al., 2016; Sun and  
245 Liang, 2020a; Sun and Liang, 2020b), which are key to accurate air quality simulations. These

246 | ~~results~~ The evaluation of CMAQ performance demonstrates the capability of CWRf-CMAQ to  
247 | credibly simulate historical air quality.

248

### 249 | **3.2 Long-term ozone trend in AQS observations**

250 | We applied a box-averaging technique (He et al., 2016b; He et al., 2019) to analyze ozone  
251 | measurements at the selected AQS monitoring sites (Fig 1). This approach used an hour by  
252 | month box to calculate the mean 24-hr diurnal cycle of ozone for each month. Then we  
253 | calculated the climatology mean over 24 hours by 12 months and the respective anomaly for  
254 | each month at each AQS site. Figure 6 shows samples of long-term mean ozone concentrations  
255 | and anomalies at four non-attainment cities: Baltimore, Maryland; Los Angeles, California;  
256 | Denver, Colorado; and New York City (NYC), New York. The hour by month climatology (left  
257 | column of Fig. 6) shows that the peak ozone concentrations in the afternoon during the ozone  
258 | season (April to September) have been reduced significantly in these cities. However, ozone  
259 | concentrations in the morning (8 am to 12 pm, all local time hereafter) and at night (8 pm to 8  
260 | am) increased slightly. These results confirm the effectiveness of recent emission controls which  
261 | were designed to reduce the peak ozone. But the expansion of ozone at moderate levels (40-50  
262 | ppbv), which are higher than the natural background of U.S. ozone (Fiore et al., 2002; Fiore et  
263 | al., 2003; Wang et al., 2009; Lefohn et al., 2014), could cause negative health impacts.

264 | The anomaly (right column of Fig. 6) shows large variabilities of ozone concentrations  
265 | because the ozone production is significantly impacted by regional climate (e.g., temperature,  
266 | precipitation) with interannual and decadal variations. Large ozone reduction occurred after 2003  
267 | when the EPA NO<sub>x</sub> State Implementation (SIP) call was implemented (He et al., 2013). The  
268 | anomalies at Los Angeles (Fig. 6b) and NYC (Fig. 6d) shows decreases of the peak ozone in the

269 afternoon of summer and increases in other times and seasons. For Baltimore and Denver, the  
270 peak ozone was not monotonically reduced, but increased in some years after 2002. Given the  
271 continuous reduction of anthropogenic emissions in the past decades, the increased ozone  
272 pollution in these areas could be caused by other factors ~~such as higher summer temperatures in~~  
273 ~~certain years or enhanced stratosphere-troposphere exchange (for Denver at the high altitude~~  
274 ~~area)~~, which need further investigations in the future.

275 We used the linear regression analysis to calculate the slope, correlation (R), and p-value  
276 of ozone trend at each local hour. Figure 7 shows ozone trends (slope, unit of ppbv/yr) at AQS  
277 sites which are statistically significant ( $R^2 > 0.5$ , and  $p < 0.05$ ) in the early morning (8 am), at  
278 noon (12 pm), in the afternoon (4 pm), and in the evening (8 pm). Consistent results with the  
279 four cities (Fig. 6) are found ubiquitously. The peak ozone at noon and in the afternoon generally  
280 had a decreasing trend in CONUS, up to 0.5 ppbv/yr, confirming the improved air quality due to  
281 regulations, while ozone in the early morning and late afternoon increased slightly at most of  
282 monitoring sites. However, AQS sites in the Bay area (San Francisco, California) and Denver  
283 had stronger positive trends in the day time. The possible explanations include the trans-pacific  
284 transport of ozone and its precursors to the U.S. West Coast (Hudman et al., 2004; Huang et al.,  
285 2010; Lin et al., 2012b) and stratosphere-troposphere exchange of ozone to high altitude region  
286 (Langford et al., 2009; Lin et al., 2012a).

### 288 **3.3. Ozone trends derived from CMAQ simulations**

289 We applied the same box-averaging technique to hourly surface ozone simulations  
290 in CONUS and conducted the linear regression analysis to estimate the ozone trend at each  
291 model grid (Fig. 8). Compared with ozone trends derived from AQS observations (Fig. 7), the

292 CMAQ model successfully captured the spatial pattern and magnitude of change in ozone  
293 pollution. For instance, at 4 pm LT, CMAQ simulated up to 0.4 ppbv/yr decrease in surface  
294 ozone in the eastern United States and south region of California state. However, CMAQ  
295 simulated statistically insignificant trends (white color in Fig. 8c) at 4 pm LT in the Bay area,  
296 Los Angeles, and Denver where AQS observations showed increasing trends (Fig. 7c). The  
297 discrepancy occurred because our model used the static chemical lateral conditions (LBCs) that  
298 did not include the change of trans-Pacific transport of air pollutants, which were known to  
299 elevate the background ozone in the West Coast. Also CMAQ does not contain stratospheric  
300 chemistry and hence cannot account the contribution of downward transport of stratospheric  
301 ozone to the high altitude region.

302 Consistent with trends derived from AQS observations, CMAQ also simulated increasing  
303 ozone trends in the early morning (8 am LT, Fig. 8a) and late afternoon (8 pm LT, Fig 8d),  
304 especially in urban regions such as Los Angeles and Chicago. He et al. (2019) found ozone  
305 increases from observations at four sites in the eastern United States and a possible cause  
306 suggested by the reduced NO-O<sub>3</sub> titration through examining the trend in odd oxygen ( $O_x = O_3 +$   
307  $NO_2$ ). Due to known interferences from nitrogen compounds such as NO<sub>x</sub> and organic nitrates to  
308 standard NO<sub>2</sub> measurements employed by EPA (Fehsenfeld et al., 1987; Dunlea et al., 2007;  
309 Dickerson et al., 2019), the analysis of O<sub>x</sub> required research grade NO<sub>2</sub> analyzer (e.g., photolytic  
310 NO<sub>2</sub> conversion) which are not available in current AQS network. Thus, our simulations provide  
311 a unique opportunity to expand such study to the whole CONUS.

312 Trends in O<sub>x</sub> concentrations simulated by CMAQ at 8 am, 12 pm, 4 pm, and 8 pm show a  
313 consistent decreasing trend over the modeling domain, up to 0.5 ppbv/yr reductions in the eastern  
314 United States (Fig. 9). The result confirms our hypothesis that the reduced NO-O<sub>3</sub> titration

315 elevated surface ozone concentrations in the early morning and late afternoon when the  
316 photochemical production of ozone is low or not active. ~~Nowadays, The-the current~~ EPA ozone  
317 standard focuses on peak ozone concentrations, i.e., MDA8 ozone which usually has maximum  
318 values at noon or in the early afternoon, so the damage from additional ozone exposure from  
319 these elevated ozone concentrations in the early morning and late afternoon is not considered  
320 under the current environment policy. These increased ozone levels could offset the benefit from  
321 reduced peak ozone in past decades, which needs further investigations to provide scientific  
322 evidence for future policy decision.

323

### 324 **3.4 Change in photochemical regime**

325 With the continuous reduction of ozone precursor emissions, changes in the complex O<sub>3</sub>-  
326 NO<sub>x</sub>-VOC chemistry are anticipated. We used the O<sub>3</sub>/NO<sub>y</sub> ratio as the indicator to study the  
327 photochemical regime change in the U.S. surface ozone production. The usage of O<sub>3</sub>/NO<sub>y</sub> ratio  
328 was first proposed by Sillman (Sillman, 1995; Sillman et al., 1997). Sillman et al. (Sillman et al.,  
329 1997) conducted a case study of observations in urban areas (Atlanta, New York, and Los  
330 Angeles) and modeling results from the Urban Airshed Model and suggested the threshold of 7  
331 as the transition region from VOC-sensitive environment to NO<sub>x</sub>-sensitive environment. Zhang  
332 et al. (2009a; 2009b) expanded this method to the CONUS with 1-year observations and CMAQ  
333 simulations (36-km spatial resolution) and suggested a threshold of 15 for ozone pollution at the  
334 national scale. In this study, we did not have access to the long-term research grade NO<sub>y</sub>  
335 observations from the AQS network and did not conduct sensitivity experiments (due to  
336 computational resource limit) with reduced NO<sub>x</sub> emissions following Sillman et al. (1997), so we  
337 have to reply on the O<sub>3</sub>/NO<sub>y</sub> threshold from literature. We conducted a simple evaluation of our

338 CMAQ results and found the threshold of 7 could be more proper for urban areas and the  
339 threshold of 15 should be more applicable for our study of the whole United State (Figure S1 in  
340 the supplementary material). Please note that the  $O_3/NO_y$  ratio could depend on the modeling  
341 framework, so due to the similarity of our modeling system (30-km CMAQ) and the model used  
342 in Zhang et al. (2009a; 2009b), our analysis suggest the similar threshold of 15.

343 The threshold of 15 proposed by Zhang et al. (2009b) was adopted to identify the VOC-  
344 sensitive or  $NO_x$ -sensitive regime, i.e.,  $O_3/NO_y < 15$  indicating the VOC-sensitive regime. For  
345 each local hour, we calculated the probability when  $O_3/NO_y$  is lower than 15 in every month.  
346 Figure 10 shows the probability of VOC-sensitive regime at 2 pm in July of 1995, 2005, and  
347 2015. Most regions dominated by the VOC-sensitive chemistry are urban or suburban where  
348 anthropogenic  $NO_x$  emissions are relatively high as compared with anthropogenic and/or  
349 biogenic VOCs emissions, such as the Los Angeles basin, the Northeast corridor (Washington  
350 D.C.-Baltimore-Philadelphia-NYC), and the Chicago metropolitan area. Noting that these maps  
351 are created based on ozone photochemical production simulated at the surface level, so the  
352 distributions are slightly different from recent studies using satellite data (Duncan et al., 2010;  
353 Jin et al., 2017; Ring et al., 2018).

354 We calculated the mean probability of VOC-sensitivity (2 pm in July) in a  $3 \times 3$  CMAQ  
355 grid in metropolitan areas of Baltimore, Los Angeles, and NYC from 1990 to 2015 (Fig. 11).  
356 CMAQ simulations suggest the transition from VOC-sensitive regime to  $NO_x$ -sensitive regime in  
357 these urban areas. There were interannual variabilities in the probability of VOC-sensitive  
358 photochemistry in Baltimore (~50%) and NYC (~80%) in the 1990s and the early 2000s. After  
359 the EPA 2003  $NO_x$  SIP call, anthropogenic  $NO_x$  emissions decreased substantially leading to  
360 reduced ozone pollution in the eastern United States (He et al., 2013), so the photochemical

361 production of surface ozone is expected to gradually become NO<sub>x</sub>-sensitive. In 2015, ozone  
362 photochemical production in Baltimore was dominated by NO<sub>x</sub> emissions (only ~20%  
363 probability of VOC-sensitive), while NYC had higher probability (>50%) of VOC-sensitive  
364 chemistry. In Los Angeles, ozone chemistry slowly leaned to NO<sub>x</sub>-sensitive, but until 2015 the  
365 local ozone production was still controlled by VOCs emissions. In regions with VOC-sensitive  
366 photochemistry in summer, reduction in NO<sub>x</sub> emissions had a limited impact on the local rate of  
367 ozone production until the photochemistry of ozone production became NO<sub>x</sub>-sensitive. Our  
368 analysis can partially explain the different responses of ozone pollution in major U.S. cities to  
369 national air quality regulations during the past decades (Cooper et al., 2012) and can provide  
370 some insights for future policy decision.

371

#### 372 **4. Conclusions and Discussion**

373 EPA AQS observations in the United States from 1990 to 2015 were analyzed to study the  
374 trend in surface ozone seasonal variations and diurnal cycles. We ~~showed~~found that the peak  
375 ozone concentrations in the afternoon decreased significantly, especially in major non-attainment  
376 regions, but the concentrations in the early morning and late afternoon increased slightly.  
377 Regional climate-air quality model captured the long-term records of U.S. ozone pollution and  
378 suggested that the increased ozone was caused by reduced NO-O<sub>3</sub> titration due to the continuous  
379 reduction of NO<sub>x</sub> emissions. Model simulations also showed changes in ozone photochemical  
380 regime. The U.S. urban/suburban areas generally transited from the VOC-sensitive regime in the  
381 early 1990s to more NO<sub>x</sub>-sensitive regime recently. But ozone production in some cities such as  
382 NYC and Los Angeles are still substantially impacted by VOC emissions. The current national  
383 and regional regulations focus on the MDA8 ozone concentrations mainly determined by the



384 peak ozone in the afternoon. Our study revealed the elevated ozone concentrations in the early  
385 morning and late afternoon which must be considered for their impacts on public health. **While**  
386 **When** NO<sub>x</sub> emissions are currently the main target of national and regional control measures, our  
387 study suggested that regulations on anthropogenic VOCs emissions could be important in certain  
388 regions. This study can improve our understanding about the effectiveness of regulations in the  
389 past decades and will provide scientific evidence for future policy decision.

390 Ozone production is highly non-linear, so accurate emissions are essential to simulate its  
391 long-term variations. Due to limited resources, we scaled the anthropogenic emissions from a  
392 baseline year (2014) to the 1990s using factors derived from the national trend data **to construct**  
393 **consistent emissions for the CONUS with respect to the EPA data**. This scaling cannot accurately  
394 reflect the detailed regional-dependent regulations for individual state such as the 2012 Health  
395 Air Act in Maryland (He et al., 2016b). Also, because the GFED data were only available after  
396 1997, the contribution of wildfire emissions to ozone pollution was not included in model  
397 simulations between 1990 to 1996. Thus, we anticipated some uncertainties in ozone simulations  
398 in the early 1990s. Our model also has limitations to reproduce ozone records in high altitude  
399 regions such as Denver because of lacking the stratospheric chemistry in CMAQ and missing the  
400 effect of stratosphere-troposphere exchange to surface ozone. Lastly, due to limited resources,  
401 our experiments used static chemical LBCs for CMAQ, which excluded the long-range transport  
402 of air pollutants into the United States. **So our current modeling system cannot take the historical**  
403 **changes of air pollution outside the United State into account. That is, the effect of long-range**  
404 **transport of air pollutants through model domain boundaries is presumed to be secondary to the**  
405 **long-term trends over the United States**. For some West Coast regions such as the state of  
406 California, the trans-Pacific transport had been enhanced in the past decades and could play a

407 | more important role in determining the local air quality. With these increased air pollutant  
408 transported into the United States, our study may underestimate the impacts of domestic  
409 emission reductions to U.S. ozone pollution, especially in the West Coast and the Southwest. To  
410 accurately evaluate the contribution from trans-boundary emission, dynamic LBCs from a global  
411 chemical transport model is needed in the future study.

412

### 413 **Author contribution**

414 H.H., X.L., and Z.T. designed the experiment; H.H. and C.S. developed the CWRP-CMAQ  
415 system and performed the CWRP modeling; Z.T. and D.T. prepared the emission data; H.H.  
416 conducted the CMAQ simulations; H.H., Z.T., and C.S. analyzed the data; H.H. prepared the  
417 manuscript with contributions from all co-authors.

418

### 419 **Acknowledgments**

420 This work was supported by the U.S. Environmental Protection Agency under Assistance  
421 Agreement No. RD-83587601. It has not been formally reviewed by EPA. The views expressed  
422 in this document are solely those of the authors and do not necessarily reflect those of the  
423 funding Agency. EPA does not endorse any products or commercial services mentioned in this  
424 publication. We thank the support of University of Illinois at Urbana-Champaign  
425 (UIUC)/USEPA award 20110150701. We thank the National Center for Supercomputing  
426 Applications (NCSA) and the National Center for Atmospheric Research (NCAR) Computation  
427 and Information System Laboratory for supercomputing support. We thank Dr. Plessel Todd for  
428 the help on the RSIG software (<https://www.epa.gov/rsig>).

429

430 **References**

431 Adams, R. M., Glyer, J. D., Johnson, S. L., and McCarl, B. A.: A reassessment of the economic-effects of ozone on  
432 United-States agriculture, *Japca-the Journal of the Air & Waste Management Association*, 39, 960-968,  
433 1989.

434 Anderson, H. R.: Air pollution and mortality: A history, *Atmospheric Environment*, 43, 142-152,  
435 10.1016/j.atmosenv.2008.09.026, 2009.

436 Appel, K. W., Napelenok, S. L., Hogrefe, C., Foley, K. M., Pouliot, G., Murphy, B. N., Luecken, D. J., and Heath,  
437 N.: Evaluation of the Community Multiscale Air Quality (CMAQ) Model Version 5.2, 2016 CMAS  
438 Conference, Chapel Hill, NC., 2016.

439 Ashmore, M. R.: Assessing the future global impacts of ozone on vegetation, *Plant Cell Environ.*, 28, 949-964,  
440 10.1111/j.1365-3040.2005.01341.x, 2005.

441 Briggs, G. A.: Chimney plumes in neutral and stable surroundings\*\*Shwartz and Tulin, *Atmospheric Environment*,  
442 19-35 (1971), *Atmospheric Environment* (1967), 6, 507-510, [https://doi.org/10.1016/0004-6981\(72\)90120-](https://doi.org/10.1016/0004-6981(72)90120-5)  
443 5, 1972.

444 Chen, L. G., Liang, X. Z., DeWitt, D., Samel, A. N., and Wang, J. X. L.: Simulation of seasonal US precipitation and  
445 temperature by the nested CWRP-ECHAM system, *Climate Dynamics*, 46, 879-896, 10.1007/s00382-015-  
446 2619-9, 2016.

447 Chou, M.-D., Suarez, M. J., Liang, X.-Z., Yan, M. M.-H., and Cote, C.: A thermal infrared radiation  
448 parameterization for atmospheric studies, 2001.

449 Cooper, O., Parrish, D., Ziemke, J., Balashov, N., Cupeiro, M., Galbally, I., Gilge, S., Horowitz, L., Jensen, N., and  
450 Lamarque, J.-F.: Global distribution and trends of tropospheric ozone: An observation-based review,  
451 *Elementa: Science of the Anthropocene*, 2, 000029, 2014.

452 Cooper, O. R., Gao, R. S., Tarasick, D., Leblanc, T., and Sweeney, C.: Long-term ozone trends at rural ozone  
453 monitoring sites across the United States, 1990-2010, *Journal of Geophysical Research-Atmospheres*, 117,  
454 D22307, 10.1029/2012jd018261, 2012.

455 Crutzen, P. J.: Photochemical reactions initiated by and influencing ozone in unpolluted tropospheric air, *Tellus*, 26,  
456 47-57, 1974.

457 Dee, D. P., Uppala, S. M., Simmons, A. J., Berrisford, P., Poli, P., Kobayashi, S., Andrae, U., Balmaseda, M. A.,  
458 Balsamo, G., Bauer, P., Bechtold, P., Beljaars, A. C. M., van de Berg, L., Bidlot, J., Bormann, N., Delsol,  
459 C., Dragani, R., Fuentes, M., Geer, A. J., Haimberger, L., Healy, S. B., Hersbach, H., Hólm, E. V., Isaksen,  
460 L., Kållberg, P., Köhler, M., Matricardi, M., McNally, A. P., Monge-Sanz, B. M., Morcrette, J. J., Park, B.  
461 K., Peubey, C., de Rosnay, P., Tavolato, C., Thépaut, J. N., and Vitart, F.: The ERA-Interim reanalysis:  
462 configuration and performance of the data assimilation system, *Q. J. R. Meteorol. Soc.*, 137, 553-597,  
463 10.1002/qj.828, 2011.

464 Dickerson, R. R., Anderson, D. C., and Ren, X.: On the use of data from commercial NOx analyzers for air pollution  
465 studies, *Atmospheric Environment*, 214, 116873, <https://doi.org/10.1016/j.atmosenv.2019.116873>, 2019.

466 Dodge, M.: *Chemistry of Oxidant Formation: Implications for Designing Effective Control Strategies U.S.*  
467 Environmental Protection Agency, Washington, D.C. EPA/600/D-87/114 (NTIS PB87179990), 1987.

468 Duncan, B. N., Yoshida, Y., Olson, J. R., Sillman, S., Martin, R. V., Lamsal, L., Hu, Y. T., Pickering, K. E., Retscher,  
469 C., Allen, D. J., and Crawford, J. H.: Application of OMI observations to a space-based indicator of NOx  
470 and VOC controls on surface ozone formation, *Atmospheric Environment*, 44, 2213-2223,  
471 10.1016/j.atmosenv.2010.03.010, 2010.

472 Dunlea, E. J., Herndon, S. C., Nelson, D. D., Volkamer, R. M., San Martini, F., Sheehy, P. M., Zahniser, M. S.,  
473 Shorter, J. H., Wormhoudt, J. C., Lamb, B. K., Allwine, E. J., Gaffney, J. S., Marley, N. A., Grutter, M.,  
474 Marquez, C., Blanco, S., Cardenas, B., Retama, A., Villegas, C. R. R., Kolb, C. E., Molina, L. T., and  
475 Molina, M. J.: Evaluation of nitrogen dioxide chemiluminescence monitors in a polluted urban  
476 environment, *Atmospheric Chemistry and Physics*, 7, 2691-2704, 2007.

477 EPA: CMAQ (Version 5.2) Scientific Document, Zenodo. <http://doi.org/10.5281/zenodo.1167892>, 2017.

478 EPA, U. S.: Air quality criteria for ozone and related photochemical oxidants, Environ. Prot. Agency, , Research  
479 Triangle Park, N.C., 2006.

480 Fehsenfeld, F. C., Dickerson, R. R., Hubler, G., Luke, W. T., Nunnermacker, L. J., Williams, E. J., Roberts, J. M.,  
481 Calvert, J. G., Curran, C. M., Delany, A. C., Eubank, C. S., Fahey, D. W., Fried, A., Gandrud, B. W.,  
482 Langford, A. O., Murphy, P. C., Norton, R. B., Pickering, K. E., and Ridley, B. A.: A ground-based  
483 intercomparison of NO, NOx, and NOy measurement techniques, *Journal of Geophysical Research-*  
484 *Atmospheres*, 92, 14710-14722, 1987.

485 Finlayson-Pitts, B. J., and Pitts, J. N.: *Chemistry of the Upper and Lower Atmosphere*, 1st ed., Academic Press, UK,

486 1999.

487 Fiore, A., Jacob, D. J., Liu, H., Yantosca, R. M., Fairlie, T. D., and Li, Q.: Variability in surface ozone background  
488 over the United States: Implications for air quality policy, *Journal of Geophysical Research: Atmospheres*,  
489 108, 10.1029/2003jd003855, 2003.

490 Fiore, A. M., Jacob, D. J., Bey, I., Yantosca, R. M., Field, B. D., Fusco, A. C., and Wilkinson, J. G.: Background  
491 ozone over the United States in summer: Origin, trend, and contribution to pollution episodes, *Journal of*  
492 *Geophysical Research: Atmospheres*, 107, ACH 11-11-ACH 11-25, 10.1029/2001jd000982, 2002.

493 Fishman, J., Ramanathan, V., Crutzen, P. J., and Liu, S. C.: Tropospheric ozone and climate, *Nature*, 282, 818-820,  
494 10.1038/282818a0, 1979.

495 He, H., Stehr, J. W., Hains, J. C., Krask, D. J., Doddridge, B. G., Vinnikov, K. Y., Canty, T. P., Hosley, K. M.,  
496 Salawitch, R. J., Worden, H. M., and Dickerson, R. R.: Trends in emissions and concentrations of air  
497 pollutants in the lower troposphere in the Baltimore/Washington airshed from 1997 to 2011, *Atmospheric*  
498 *Chemistry and Physics*, 13, 7859-7874, 10.5194/acp-13-7859-2013, 2013.

499 He, H., Liang, X.-Z., Lei, H., and Wuebbles, D. J.: Future U.S. ozone projections dependence on regional emissions,  
500 climate change, long-range transport and differences in modeling design, *Atmospheric Environment*, 128,  
501 124-133, <https://doi.org/10.1016/j.atmosenv.2015.12.064>, 2016a.

502 He, H., Vinnikov, K. Y., Li, C., Krotkov, N. A., Jongeward, A. R., Li, Z. Q., Stehr, J. W., Hains, J. C., and Dickerson,  
503 R. R.: Response of SO<sub>2</sub> and particulate air pollution to local and regional emission controls: A case study in  
504 Maryland, *Earth Future*, 4, 94-109, 10.1002/2015ef000330, 2016b.

505 He, H., Liang, X. Z., and Wuebbles, D. J.: Effects of emissions change, climate change and long-range transport on  
506 regional modeling of future US particulate matter pollution and speciation, *Atmospheric Environment*, 179,  
507 166-176, 10.1016/j.atmosenv.2018.02.020, 2018.

508 He, H., Vinnikov, K. Y., Krotkov, N. A., Edgerton, E. S., Schwab, J. J., and Dickerson, R. R.: Chemical climatology  
509 of atmospheric pollutants in the eastern United States: Seasonal/diurnal cycles and contrast under  
510 clear/cloudy conditions for remote sensing, *Atmospheric Environment*, 206, 85-107,  
511 <https://doi.org/10.1016/j.atmosenv.2019.03.003>, 2019.

512 Hogrefe, C., Hao, W., Zalewsky, E. E., Ku, J. Y., Lynn, B., Rosenzweig, C., Schultz, M. G., Rast, S., Newchurch, M.  
513 J., Wang, L., Kinney, P. L., and Sistla, G.: An analysis of long-term regional-scale ozone simulations over  
514 the Northeastern United States: variability and trends, *Atmospheric Chemistry and Physics*, 11, 567-582,  
515 10.5194/acp-11-567-2011, 2011.

516 Holton, J. R., Haynes, P. H., McIntyre, M. E., Douglass, A. R., Rood, R. B., and Pfister, L.: Stratosphere-troposphere  
517 exchange, *Reviews of Geophysics*, 33, 403-439, 10.1029/95rg02097, 1995.

518 Holtslag, A. A. M., and Boville, B. A.: Local Versus Nonlocal Boundary-Layer Diffusion in a Global Climate  
519 Model, *Journal of Climate*, 6, 1825-1842, 10.1175/1520-0442(1993)006<1825:lvnbl>2.0.co;2, 1993.

520 Houyoux, M. R., Vukovich, J. M., Coats Jr., C. J., Wheeler, N. J. M., and Kasibhatla, P. S.: Emission inventory  
521 development and processing for the Seasonal Model for Regional Air Quality (SMRAQ) project, *Journal of*  
522 *Geophysical Research: Atmospheres*, 105, 9079-9090, 10.1029/1999jd900975, 2000.

523 Huang, H. C., Liang, X. Z., Kunkel, K. E., Caughey, M., and Williams, A.: Seasonal simulation of tropospheric  
524 ozone over the midwestern and northeastern United States: An application of a coupled regional climate  
525 and air quality modeling system, *J. Appl. Meteorol. Climatol.*, 46, 945-960, 10.1175/jam2521.1, 2007.

526 Huang, M., Carmichael, G., Adhikary, B., Spak, S., Kulkarni, S., Cheng, Y., Wei, C., Tang, Y., Parrish, D., and  
527 Oltmans, S.: Impacts of transported background ozone on California air quality during the ARCTAS-CARB  
528 period—a multi-scale modeling study, *Atmospheric Chemistry and Physics*, 10, 6947-6968, 2010.

529 Hudman, R., Jacob, D. J., Cooper, O., Evans, M., Heald, C., Park, R., Fehsenfeld, F., Flocke, F., Holloway, J., and  
530 Hübler, G.: Ozone production in transpacific Asian pollution plumes and implications for ozone air quality  
531 in California, *Journal of Geophysical Research: Atmospheres*, 109, 2004.

532 IPCC: Climate Change 2013: The Physical Science Basis., Contribution of Working Group I to the Fifth Assessment  
533 Report (AR5) of the Intergovernmental Panel on Climate Change, 1535 pp.,  
534 doi:10.1017/CBO9781107415324, 2013.

535 Jacob, D. J.: Heterogeneous chemistry and tropospheric ozone, *Atmospheric Environment*, 34, 2131-2159,  
536 10.1016/s1352-2310(99)00462-8, 2000.

537 Jaffe, D., and Ray, J.: Increase in surface ozone at rural sites in the western US, *Atmospheric Environment*, 41,  
538 5452-5463, 10.1016/j.atmosenv.2007.02.34, 2007.

539 Jerrett, M., Burnett, R. T., Pope, C. A., Ito, K., Thurston, G., Krewski, D., Shi, Y., Calle, E., and Thun, M.: Long-  
540 Term Ozone Exposure and Mortality, *N. Engl. J. Med.*, 360, 1085-1095, 10.1056/NEJMoa0803894, 2009.

541 Jin, X., Fiore, A. M., Murray, L. T., Valin, L. C., Lamsal, L. N., Duncan, B., Folkert Boersma, K., De Smedt, I.,

542 Abad, G. G., Chance, K., and Tonnesen, G. S.: Evaluating a Space-Based Indicator of Surface Ozone-NOx-  
543 VOC Sensitivity Over Midlatitude Source Regions and Application to Decadal Trends, *Journal of*  
544 *Geophysical Research: Atmospheres*, 122, 10,439-410,461, doi:10.1002/2017JD026720, 2017.

545 Kleinman, L. I.: Low and high NOx tropospheric photochemistry, *Journal of Geophysical Research-Atmospheres*,  
546 99, 16831-16838, 10.1029/94jd01028, 1994.

547 Langford, A., Aikin, K., Eubank, C., and Williams, E.: Stratospheric contribution to high surface ozone in Colorado  
548 during springtime, *Geophysical Research Letters*, 36, 2009.

549 Lefohn, A. S., Shadwick, D., and Oltmans, S. J.: Characterizing long-term changes in surface ozone levels in the  
550 United States (1980-2005), *Atmospheric Environment*, 42, 8252-8262, 10.1016/j.atmosenv.2008.07.060,  
551 2008.

552 Lefohn, A. S., Shadwick, D., and Oltmans, S. J.: Characterizing changes in surface ozone levels in metropolitan and  
553 rural areas in the United States for 1980-2008 and 1994-2008, *Atmospheric Environment*, 44, 5199-5210,  
554 10.1016/j.atmosenv.2010.08.049, 2010.

555 Lefohn, A. S., Emery, C., Shadwick, D., Wernli, H., Jung, J., and Oltmans, S. J.: Estimates of background surface  
556 ozone concentrations in the United States based on model-derived source apportionment, *Atmospheric*  
557 *Environment*, 84, 275-288, <https://doi.org/10.1016/j.atmosenv.2013.11.033>, 2014.

558 Levy, H., Mahlman, J. D., Moxim, W. J., and Liu, S. C.: Tropospheric ozone - the role of transport, *Journal of*  
559 *Geophysical Research-Atmospheres*, 90, 3753-3772, 10.1029/JD090iD02p03753, 1985.

560 Liang, X.-Z., Xu, M., Yuan, X., Ling, T., Choi, H. I., Zhang, F., Chen, L., Liu, S., Su, S., Qiao, F., He, Y., Wang, J.  
561 X. L., Kunkel, K. E., Gao, W., Joseph, E., Morris, V., Yu, T.-W., Dudhia, J., and Michalakes, J.: Regional  
562 Climate-Weather Research and Forecasting Model, *Bulletin of the American Meteorological Society*, 93,  
563 1363-1387, 10.1175/bams-d-11-00180.1, 2012.

564 Liang, X.-Z., Sun, C., Zheng, X., Dai, Y., Xu, M., Choi, H. I., Ling, T., Qiao, F., Kong, X., Bi, X., Song, L., and  
565 Wang, F.: CWRF performance at downscaling China climate characteristics, *Climate Dynamics*, 52, 2159-  
566 2184, 10.1007/s00382-018-4257-5, 2019.

567 Lin, M., Fiore, A. M., Cooper, O. R., Horowitz, L. W., Langford, A. O., Levy, H., Johnson, B. J., Naik, V., Oltmans,  
568 S. J., and Senff, C. J.: Springtime high surface ozone events over the western United States: Quantifying  
569 the role of stratospheric intrusions, *Journal of Geophysical Research: Atmospheres*, 117, 2012a.

570 Lin, M., Fiore, A. M., Horowitz, L. W., Cooper, O. R., Naik, V., Holloway, J., Johnson, B. J., Middlebrook, A. M.,  
571 Oltmans, S. J., and Pollack, I. B.: Transport of Asian ozone pollution into surface air over the western  
572 United States in spring, *Journal of Geophysical Research: Atmospheres*, 117, 2012b.

573 Liu, S., Wang, J. X. L., Liang, X.-Z., and Morris, V.: A hybrid approach to improving the skills of seasonal climate  
574 outlook at the regional scale, *Climate Dynamics*, 46, 483-494, 10.1007/s00382-015-2594-1, 2016.

575 Logan, J. A., Prather, M. J., Wofsy, S. C., and McElroy, M. B.: Tropospheric chemistry - a global perspective,  
576 *Journal of Geophysical Research-Oceans and Atmospheres*, 86, 7210-7254, 10.1029/JC086iC08p07210,  
577 1981.

578 Oltmans, S. J., Lefohn, A. S., Harris, J. M., Galbally, I., Scheel, H. E., Bodeker, G., Brunke, E., Claude, H., Tarasick,  
579 D., Johnson, B. J., Simmonds, P., Shadwick, D., Anlauf, K., Hayden, K., Schmidlin, F., Fujimoto, T., Akagi,  
580 K., Meyer, C., Nichol, S., Davies, J., Redondas, A., and Cuevas, E.: Long-term changes in tropospheric  
581 ozone, *Atmospheric Environment*, 40, 3156-3173, 10.1016/j.atmosenv.2006.01.029, 2006.

582 Peng, Y. P., Chen, K. S., Wang, H. K., and Lai, C. H.: In Situ Measurements of Hydrogen Peroxide, Nitric Acid and  
583 Reactive Nitrogen to Assess the Ozone Sensitivity in Pingtung County, Taiwan, *Aerosol and Air Quality*  
584 *Research*, 11, 59-69, 10.4209/aaqr.2010.10.0091, 2011.

585 Pour-Biazar, A., Khan, M., Wang, L. H., Park, Y. H., Newchurch, M., McNider, R. T., Liu, X., Byun, D. W., and  
586 Cameron, R.: Utilization of satellite observation of ozone and aerosols in providing initial and boundary  
587 condition for regional air quality studies, *Journal of Geophysical Research-Atmospheres*, 116, D18309,  
588 10.1029/2010jd015200, 2011.

589 Qiao, F., and Liang, X.-Z.: Effects of cumulus parameterization closures on simulations of summer precipitation  
590 over the continental United States, *Climate Dynamics*, 49, 225-247, 10.1007/s00382-016-3338-6, 2017.

591 Qiao, F. X., and Liang, X. Z.: Effects of cumulus parameterizations on predictions of summer flood in the Central  
592 United States, *Climate Dynamics*, 45, 727-744, 10.1007/s00382-014-2301-7, 2015.

593 Qiao, F. X., and Liang, X. Z.: Effects of cumulus parameterization closures on simulations of summer precipitation  
594 over the United States coastal oceans, *J. Adv. Model. Earth Syst.*, 8, 764-785, 10.1002/2015ms000621,  
595 2016.

596 Ramanathan, V., and Dickinson, R. E.: Role of stratospheric ozone in the zonal and seasonal radiative energy-  
597 balance of the Earth-troposphere system, *Journal of the Atmospheric Sciences*, 36, 1084-1104, 1979.

598 Randerson, J. T., Van Der Werf, G. R., Giglio, L., Collatz, G. J., and Kasibhatla, P. S.: Global Fire Emissions  
599 Database, Version 4.1 (GFEDv4). ORNL Distributed Active Archive Center, 2017.

600 Ring, A. M., Canty, T. P., Anderson, D. C., Vinciguerra, T. P., He, H., Goldberg, D. L., Ehrman, S. H., Dickerson, R.  
601 R., and Salawitch, R. J.: Evaluating commercial marine emissions and their role in air quality policy using  
602 observations and the CMAQ model, *Atmospheric Environment*, 173, 96-107,  
603 <https://doi.org/10.1016/j.atmosenv.2017.10.037>, 2018.

604 Seinfeld, J. H., and Pandis, S. N.: *Atmospheric Chemistry and Physics: From Air Pollution to Climate Change*, 2nd  
605 ed., John Wiley & Sons, Inc., 2006.

606 Seinfeld, J. H. e. a.: *Rethinking the Ozone Problem in Urban and Regional Air Pollution*, National Academics Press,  
607 Washington, DC, 1991.

608 Shon, Z.-H., Lee, G., Song, S.-K., Lee, M., Han, J., and Lee, D.: Characteristics of reactive nitrogen compounds and  
609 other relevant trace gases in the atmosphere at urban and rural areas of Korea during May–June, 2004,  
610 *Journal of Atmospheric Chemistry*, 58, 203-218, 10.1007/s10874-007-9088-4, 2007.

611 Sillman, S.: The use of NO<sub>y</sub>, H<sub>2</sub>O<sub>2</sub>, and HNO<sub>3</sub> as indicators for ozone-NO<sub>x</sub>-hydrocarbon sensitivity in urban  
612 locations, *Journal of Geophysical Research-Atmospheres*, 100, 14175-14188, 10.1029/94jd02953, 1995.

613 Sillman, S., He, D., Cardelino, C., and Imhoff, R. E.: The Use of Photochemical Indicators to Evaluate Ozone-NO<sub>x</sub>-  
614 Hydrocarbon Sensitivity: Case Studies from Atlanta, New York, and Los Angeles, *J. Air Waste Manage.*  
615 *Assoc.*, 47, 1030-1040, 10.1080/10962247.1997.11877500, 1997.

616 Sillman, S.: The relation between ozone, NO<sub>x</sub> and hydrocarbons in urban and polluted rural environments,  
617 *Atmospheric Environment*, 33, 1821-1845, 10.1016/s1352-2310(98)00345-8, 1999.

618 Sillman, S., and He, D.: Some theoretical results concerning O<sub>3</sub>-NO<sub>x</sub>-VOC chemistry and NO<sub>x</sub>-VOC indicators,  
619 *Journal of Geophysical Research: Atmospheres*, 107, ACH 26-21-ACH 26-15, 10.1029/2001jd001123,  
620 2002.

621 Skamarock, W. C., Klemp, J. B., Dudhia, J., Gill, D. O., Barker, D. M., Duda, M. G., Huang, X.-Y., Wang, W., and  
622 Powers, J. G.: A Description of the Advanced Research WRF Version 3, NCAR Technical Note,  
623 NCAR/TN-475+STR, 113 pp, 2008.

624 Stevenson, D. S., Dentener, F. J., Schultz, M. G., Ellingsen, K., van Noije, T. P. C., Wild, O., Zeng, G., Amann, M.,  
625 Atherton, C. S., Bell, N., Bergmann, D. J., Bey, I., Butler, T., Cofala, J., Collins, W. J., Derwent, R. G.,  
626 Doherty, R. M., Drevet, J., Eskes, H. J., Fiore, A. M., Gauss, M., Hauglustaine, D. A., Horowitz, L. W.,  
627 Isaksen, I. S. A., Krol, M. C., Lamarque, J. F., Lawrence, M. G., Montanaro, V., Muller, J. F., Pitari, G.,  
628 Prather, M. J., Pyle, J. A., Rast, S., Rodriguez, J. M., Sanderson, M. G., Savage, N. H., Shindell, D. T.,  
629 Strahan, S. E., Sudo, K., and Szopa, S.: Multimodel ensemble simulations of present-day and near-future  
630 tropospheric ozone, *Journal of Geophysical Research-Atmospheres*, 111, D08301, 10.1029/2005jd006338,  
631 2006.

632 Sun, C., and Liang, X. Z.: Improving U.S. extreme precipitation simulation: Dependence on cumulus  
633 parameterization and underlying mechanism, *Climate Dynamics*, to be submitted, 2020a.

634 Sun, C., and Liang, X. Z.: Improving U.S. extreme precipitation simulation: Sensitivity to physics parameterizations,  
635 *Climate Dynamics*, to be submitted, 2020b.

636 Tagaris, E., Manomaiphiboon, K., Liao, K.-J., Leung, L. R., Woo, J.-H., He, S., Amar, P., and Russell, A. G.:  
637 Impacts of global climate change and emissions on regional ozone and fine particulate matter  
638 concentrations over the United States, *Journal of Geophysical Research: Atmospheres*, 112,  
639 doi:10.1029/2006JD008262, 2007.

640 Tang, Y., Lee, P., Tsidulko, M., Huang, H.-C., McQueen, J. T., DiMego, G. J., Emmons, L. K., Pierce, R. B.,  
641 Thompson, A. M., Lin, H.-M., Kang, D., Tong, D., Yu, S., Mathur, R., Pleim, J. E., Otte, T. L., Pouliot, G.,  
642 Young, J. O., Schere, K. L., Davidson, P. M., and Stajner, I.: The impact of chemical lateral boundary  
643 conditions on CMAQ predictions of tropospheric ozone over the continental United States, *Environmental*  
644 *Fluid Mechanics*, 9, 43-58, 10.1007/s10652-008-9092-5, 2009.

645 Tao, W.-K., Simpson, J., and McCumber, M.: An Ice-Water Saturation Adjustment, *Mon. Weather Rev.*, 117, 231-  
646 235, 10.1175/1520-0493(1989)117<0231:aiwsa>2.0.co;2, 1989.

647 Tong, D., Pan, L., Chen, W., Lamsal, L., Lee, P., Tang, Y., Kim, H., Kondragunta, S., and Stajner, I.: Impact of the  
648 2008 Global Recession on air quality over the United States: Implications for surface ozone levels from  
649 changes in NO<sub>x</sub> emissions, *Geophysical Research Letters*, 43, 9280-9288, 10.1002/2016gl069885, 2016.

650 Tong, D. Q., Lamsal, L., Pan, L., Ding, C., Kim, H., Lee, P., Chai, T. F., Pickering, K. E., and Stajner, I.: Long-term  
651 NO<sub>x</sub> trends over large cities in the United States during the great recession: Comparison of satellite  
652 retrievals, ground observations, and emission inventories, *Atmospheric Environment*, 107, 70-84,  
653 10.1016/j.atmosenv.2015.01.035, 2015.

654 Tonnesen, G. S., and Dennis, R. L.: Analysis of radical propagation efficiency to assess ozone sensitivity to  
655 hydrocarbons and NO<sub>x</sub> : 1. Local indicators of instantaneous odd oxygen production sensitivity, *Journal of*  
656 *Geophysical Research: Atmospheres*, 105, 9213-9225, 10.1029/1999jd900371, 2000a.

657 Tonnesen, G. S., and Dennis, R. L.: Analysis of radical propagation efficiency to assess ozone sensitivity to  
658 hydrocarbons and NO<sub>x</sub> : 2. Long-lived species as indicators of ozone concentration sensitivity, *Journal of*  
659 *Geophysical Research: Atmospheres*, 105, 9227-9241, 10.1029/1999jd900372, 2000b.

660 van der Werf, G. R., Randerson, J. T., Giglio, L., van Leeuwen, T. T., Chen, Y., Rogers, B. M., Mu, M. Q., van  
661 Marle, M. J. E., Morton, D. C., Collatz, G. J., Yokelson, R. J., and Kasibhatla, P. S.: Global fire emissions  
662 estimates during 1997-2016, *Earth Syst. Sci. Data*, 9, 697-720, 10.5194/essd-9-697-2017, 2017.

663 Wang, H., Jacob, D. J., Le Sager, P., Streets, D. G., Park, R. J., Gilliland, A. B., and van Donkelaar, A.: Surface  
664 ozone background in the United States: Canadian and Mexican pollution influences, *Atmospheric*  
665 *Environment*, 43, 1310-1319, <https://doi.org/10.1016/j.atmosenv.2008.11.036>, 2009.

666 WHO: Health aspects of air pollution with particulate matter, ozone and nitrogen dioxide, *World Health*  
667 *Organisation, Bonn*, 2003.

668 Xie, Y., Elleman, R., Jobson, T., and Lamb, B.: Evaluation of O<sub>3</sub>-NO<sub>x</sub>-VOC sensitivities predicted with the CMAQ  
669 photochemical model using Pacific Northwest 2001 field observations, *Journal of Geophysical Research:*  
670 *Atmospheres*, 116, 10.1029/2011jd015801, 2011.

671 Xu, K.-M., and Randall, D. A.: A Semiempirical Cloudiness Parameterization for Use in Climate Models, *Journal of*  
672 *the Atmospheric Sciences*, 53, 3084-3102, 10.1175/1520-0469(1996)053<3084:ascpfu>2.0.co;2, 1996.

673 Yarwood, G. S., Whitten, G. Z., Jung, J., Heo, G., and Allen, D.: Development, Evaluation and Testing of Version 6  
674 of the Carbon Bond Chemical Mechanism (CB6),  
675 [https://www.tceq.texas.gov/assets/public/implementation/air/am/contracts/reports/pm/5820784005FY1026-](https://www.tceq.texas.gov/assets/public/implementation/air/am/contracts/reports/pm/5820784005FY1026-20100922-environ-cb6.pdf)  
676 [20100922-environ-cb6.pdf](https://www.tceq.texas.gov/assets/public/implementation/air/am/contracts/reports/pm/5820784005FY1026-20100922-environ-cb6.pdf), 2010.

677 Yuan, X., and Liang, X. Z.: Improving cold season precipitation prediction by the nested CWRP-CFS system,  
678 *Geophysical Research Letters*, 38, L02706, 10.1029/2010gl046104, 2011.

679 Zhang, Y., Vijayaraghavan, K., Wen, X. Y., Snell, H. E., and Jacobson, M. Z.: Probing into regional ozone and  
680 particulate matter pollution in the United States: 1. A 1 year CMAQ simulation and evaluation using  
681 surface and satellite data, *Journal of Geophysical Research-Atmospheres*, 114, 10.1029/2009jd011898,  
682 2009a.

683 Zhang, Y., Wen, X. Y., Wang, K., Vijayaraghavan, K., and Jacobson, M. Z.: Probing into regional O<sub>3</sub> and particulate  
684 matter pollution in the United States: 2. An examination of formation mechanisms through a process  
685 analysis technique and sensitivity study, *Journal of Geophysical Research-Atmospheres*, 114,  
686 10.1029/2009jd011900, 2009b.

687 Zhu, J. H., and Liang, X. Z.: Impacts of the Bermuda High on Regional Climate and Ozone over the United States,  
688 *Journal of Climate*, 26, 1018-1032, 10.1175/jcli-d-12-00168.1, 2013.

689  
690

691 **Tables and Figures**

692

693 **Table 1.** Summary of multiyear mean average of daily CO, NO<sub>x</sub>, and NMVOCs emissions in the  
 694 CONUS and five subdomains. (Unit: mol/km<sup>2</sup> per second) Please note that our California and  
 695 Texas subdomains include more area than the states of California and Texas.  
 696

<b>CONUS</b>				<b>Southeast</b>		
Year	CO	NO <sub>x</sub>	NMVOCs	CO	NO <sub>x</sub>	NMVOCs
1990-1994	32.9	1.24	0.94	47.2	1.43	1.03
1995-1999	26.2	1.18	0.76	37.4	1.36	0.85
2000-2004	18.9	1.26	0.69	26.4	1.46	0.72
2005-2009	12.3	0.94	0.60	16.9	1.07	0.59
2010-2015	8.0	0.60	0.46	11.0	0.66	0.45
<b>California</b>				<b>Northeast</b>		
1990-1994	18.3	1.22	0.57	110.3	3.29	2.12
1995-1999	14.6	1.16	0.46	87.2	3.16	1.68
2000-2004	10.6	1.23	0.40	62.1	3.41	1.43
2005-2009	7.1	0.91	0.35	40.3	2.56	1.25
2010-2015	4.6	0.56	0.26	25.9	1.62	0.93
<b>Texas</b>				<b>Midwest</b>		
1990-1994	22.6	1.21	1.26	58.2	1.88	1.41
1995-1999	18.1	1.15	1.03	46.3	1.80	1.14
2000-2004	13.0	1.20	1.01	33.4	1.92	0.98
2005-2009	8.4	0.91	0.92	22.0	1.44	0.85
2010-2015	5.5	0.60	0.73	14.3	0.91	0.63

697



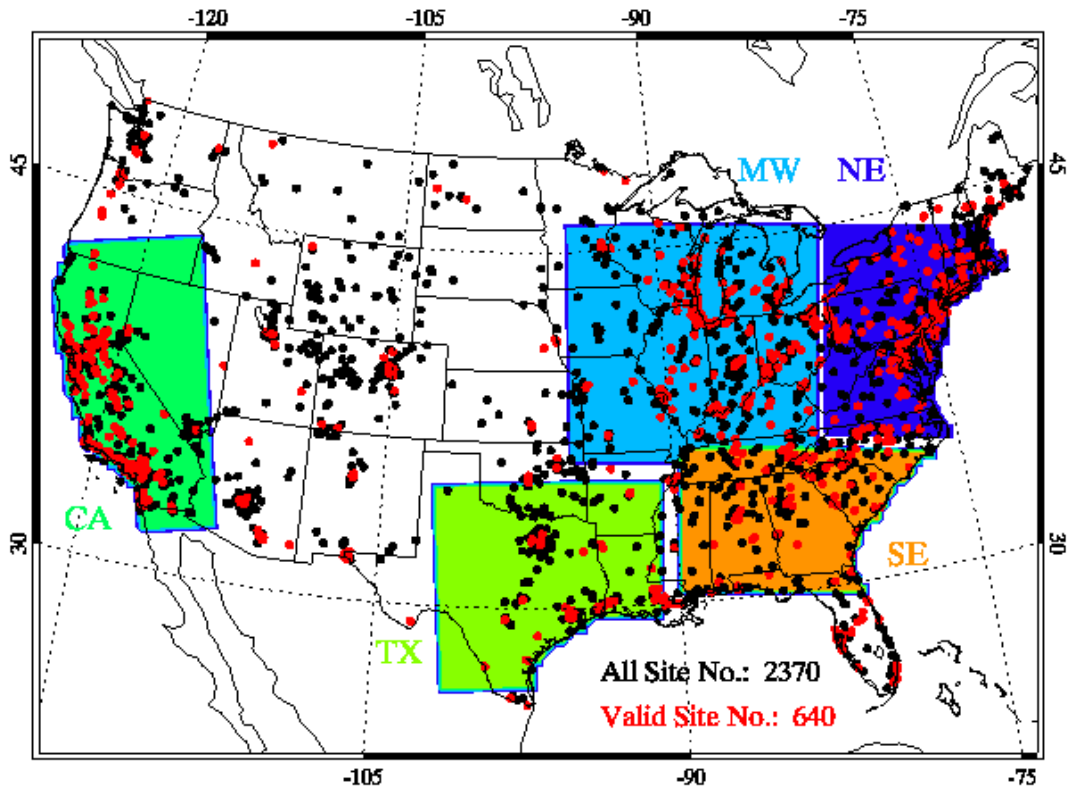
698 **Table 2.** Summary about the comparison of JJA MDA8 ozone concentrations from AQS  
699 observations and CMAQ simulations during 2000-2015 in the CONUS and subdomains. Slope  
700 and Correlation (Corr. R) are calculated for each year based on linear regression analysis. Please  
701 note that our California and Texas subdomains include more area than the states of California  
702 and Texas.  
703

Year	Slope	Corr. R	NMB	RMSE	Year	Slope	Corr. R	NMB	RMSE
<b>CONUS</b>									
<b>2000</b>	0.73	0.37	-6.9	10.5	<b>2008</b>	0.70	0.54	-5.4	8.4
<b>2001</b>	0.80	0.61	-7.7	8.7	<b>2009</b>	0.78	0.35	-1.6	8.5
<b>2002</b>	0.71	0.63	-8.6	9.2	<b>2010</b>	0.75	0.51	-6.2	8.4
<b>2003</b>	0.81	0.60	-4.3	8.4	<b>2011</b>	0.77	0.42	-7.1	9.2
<b>2004</b>	0.85	0.39	1.3	8.9	<b>2012</b>	0.67	0.60	-10.7	9.3
<b>2005</b>	0.87	0.54	-7.3	8.8	<b>2013</b>	0.70	0.50	-1.8	7.9
<b>2006</b>	0.77	0.48	-7.6	9.1	<b>2014</b>	0.72	0.44	-3.0	7.6
<b>2007</b>	0.70	0.60	-6.1	8.0	<b>2015</b>	0.73	0.41	-4.2	7.7
<b>California</b>									
<b>2000</b>	0.70	0.67	-19.3	15.2	<b>2008</b>	0.63	0.53	-18.0	14.8
<b>2001</b>	0.72	0.63	-18.1	14.8	<b>2009</b>	0.67	0.61	-19.0	13.5
<b>2002</b>	0.80	0.55	-15.5	14.4	<b>2010</b>	0.62	0.55	-19.0	14.1
<b>2003</b>	0.80	0.55	-20.1	16.2	<b>2011</b>	0.68	0.57	-17.0	13.3
<b>2004</b>	0.78	0.51	-19.2	16.1	<b>2012</b>	0.64	0.63	-21.4	14.9
<b>2005</b>	0.78	0.54	-19.0	15.3	<b>2013</b>	0.64	0.60	-17.9	13.5
<b>2006</b>	0.80	0.61	-20.5	15.6	<b>2014</b>	0.69	0.56	-21.9	14.8
<b>2007</b>	0.69	0.65	-16.0	12.9	<b>2015</b>	0.72	0.61	-22.3	14.2
<b>Texas</b>									
<b>2000</b>	0.60	0.77	-20.4	11.8	<b>2008</b>	0.62	0.74	-10.5	6.6
<b>2001</b>	0.58	0.62	-19.6	11.5	<b>2009</b>	0.73	0.78	-17.1	8.7
<b>2002</b>	0.70	0.72	-10.4	6.6	<b>2010</b>	0.65	0.77	-9.4	5.3
<b>2003</b>	0.64	0.78	-8.8	6.5	<b>2011</b>	0.52	0.83	-22.7	12.1
<b>2004</b>	0.97	0.55	-7.2	5.8	<b>2012</b>	0.53	0.86	-17.8	9.4
<b>2005</b>	0.70	0.78	-21.5	11.4	<b>2013</b>	0.53	0.74	-11.6	6.9
<b>2006</b>	0.66	0.83	-20.5	11.3	<b>2014</b>	0.66	0.72	-5.0	4.7
<b>2007</b>	0.77	0.84	-4.0	3.9	<b>2015</b>	0.76	0.61	-10.1	5.8
<b>Southeast</b>									
<b>2000</b>	0.61	0.41	-20.5	13.3	<b>2008</b>	0.52	0.77	-13.4	8.3
<b>2001</b>	0.64	0.70	-7.7	6.2	<b>2009</b>	0.88	0.52	-2.7	4.2

<b>2002</b>	0.56	0.77	-14.1	9.5	<b>2010</b>	0.69	0.75	-7.8	5.1
<b>2003</b>	0.65	0.77	-0.7	4.7	<b>2011</b>	0.84	0.62	-13.5	8.2
<b>2004</b>	0.81	0.59	3.2	4.4	<b>2012</b>	0.62	0.73	-9.4	6.1
<b>2005</b>	0.54	0.64	-8.8	6	<b>2013</b>	0.74	0.70	7.0	4.1
<b>2006</b>	0.74	0.60	-14	9	<b>2014</b>	0.84	0.40	0.9	4.0
<b>2007</b>	0.56	0.71	-14.1	9	<b>2015</b>	0.71	0.44	-2.6	4.2
<b>Northeast</b>									
<b>2000</b>	0.50	0.25	7.9	7.0	<b>2008</b>	0.46	0.11	-0.5	5.8
<b>2001</b>	0.46	0.28	-3.6	6.0	<b>2009</b>	0.67	0.23	13.7	7.3
<b>2002</b>	0.51	0.13	-8.5	8.3	<b>2010</b>	0.49	0.10	-0.4	5.6
<b>2003</b>	0.85	0.16	3.0	5.3	<b>2011</b>	0.47	0.31	3.2	5.9
<b>2004</b>	0.81	0.21	10.0	6.6	<b>2012</b>	0.55	0.17	-2.9	5.3
<b>2005</b>	0.84	0.11	2.5	5.8	<b>2013</b>	0.78	0.45	11.6	6.4
<b>2006</b>	0.45	0.21	3.0	6.0	<b>2014</b>	0.60	0.33	-4.8	5.1
<b>2007</b>	0.48	0.19	-0.7	5.6	<b>2015</b>	0.49	0.11	2.2	5.1
<b>Midwest</b>									
<b>2000</b>	0.41	0.25	3.4	5.9	<b>2008</b>	0.44	0.25	3.5	4.7
<b>2001</b>	0.55	0.30	-2.3	4.9	<b>2009</b>	0.54	0.22	14	7.2
<b>2002</b>	0.45	0.27	-5.2	7.0	<b>2010</b>	0.57	0.12	2.4	5.3
<b>2003</b>	0.66	0.25	-0.1	4.7	<b>2011</b>	0.45	0.21	1.1	5.6
<b>2004</b>	0.68	0.44	13.9	7.5	<b>2012</b>	0.46	0.19	-11.6	8.3
<b>2005</b>	0.76	0.15	-4.4	5.6	<b>2013</b>	0.74	0.18	4.9	4.0
<b>2006</b>	0.50	0.17	0.3	5.0	<b>2014</b>	0.64	0.20	5.7	4.1
<b>2007</b>	0.39	0.20	-0.6	5.6	<b>2015</b>	0.68	0.27	8.7	4.7

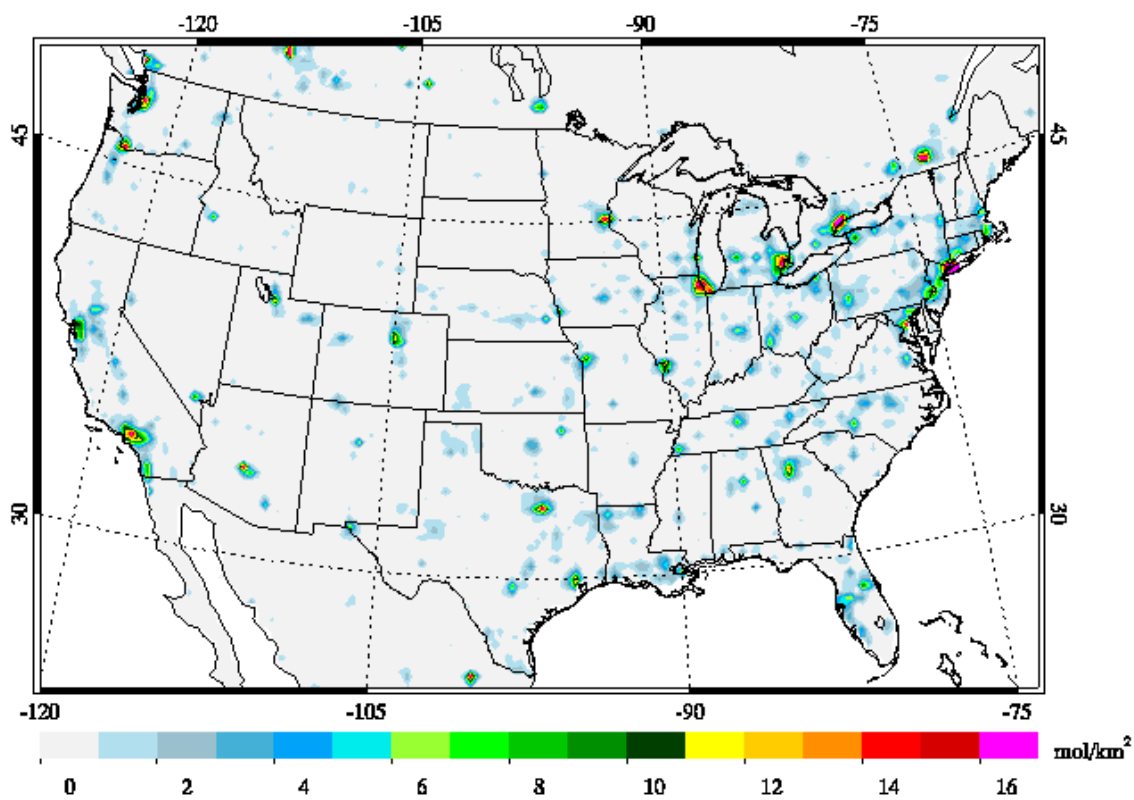
704 NMB: Normalized Mean Bias (Unit: %)  
705 RMSE: Root Mean Square Error (Unit: ppbv)  
706

707 **Figure 1.** Locations of EPA AQS sites for surface ozone monitoring during 1990-2015. Red dots  
708 stand for monitoring sites with more than 20 year record. Black dots show the locations of  
709 monitoring sites have short data records which are not used in this study. The map shows the  
710 CWRf-CMAQ 30-km domain and five subdomains sensitive to air pollution. CA: California  
711 (including nearby parts of Nevada, Arizona and Oregon); TX: Texas (including nearby parts of  
712 Louisiana, Arkansas, and Oklahoma); SE: Southeast; NE: Northeast; MW: Midwest. Please note  
713 that our CA and TX subdomains include more area than the states of California and Texas.



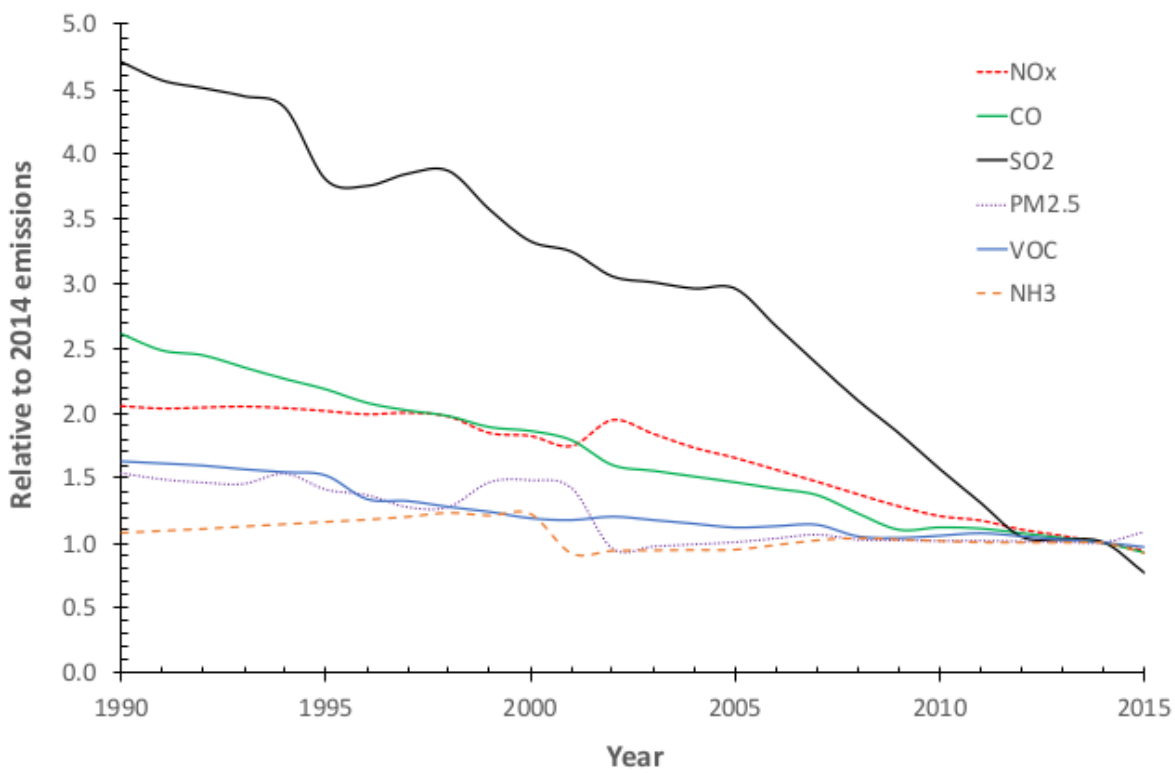
714

715 **Figure 2.** Averaged daily NO<sub>x</sub> emissions between 2010 and 2015 in the modeling domain (Unit:  
716 mol/km<sup>2</sup> per second).



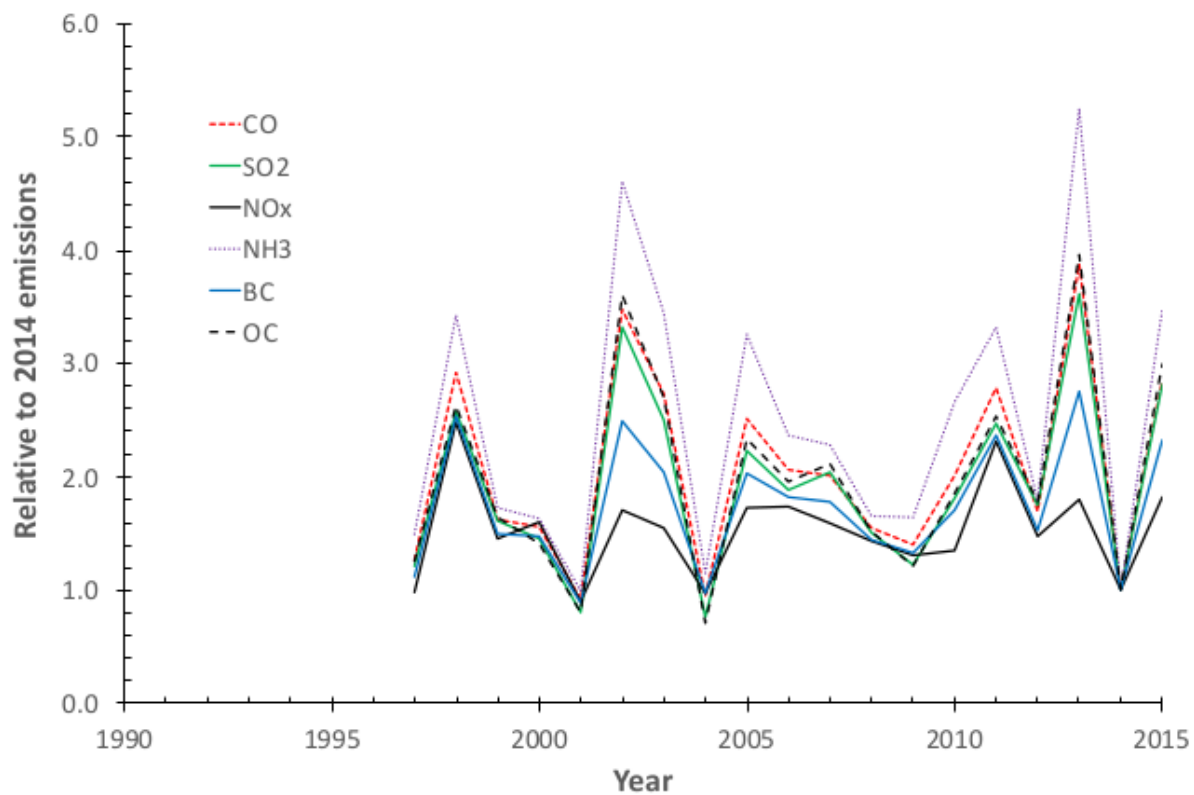
717

718 **Figure 3.** Anthropogenic emission evolution relative to 2014 in the modeling domain from 1990  
719 – 2015.



720  
721

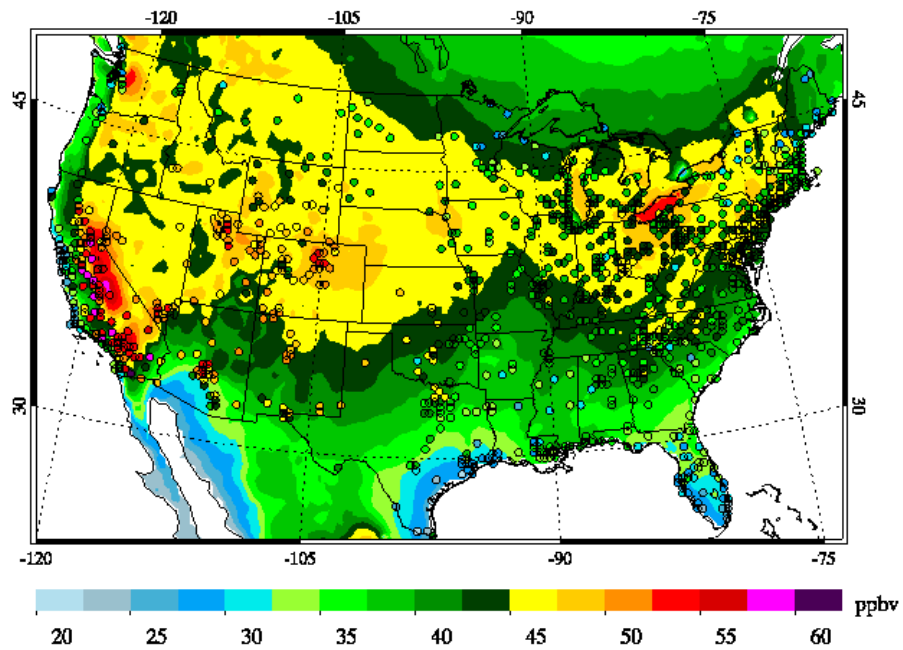
722 **Figure 4.** Fire emission evolution relative to 2014 in the modeling domain from 1990 – 2015.  
723 Noting that GFED fire emissions are not available before 1997.



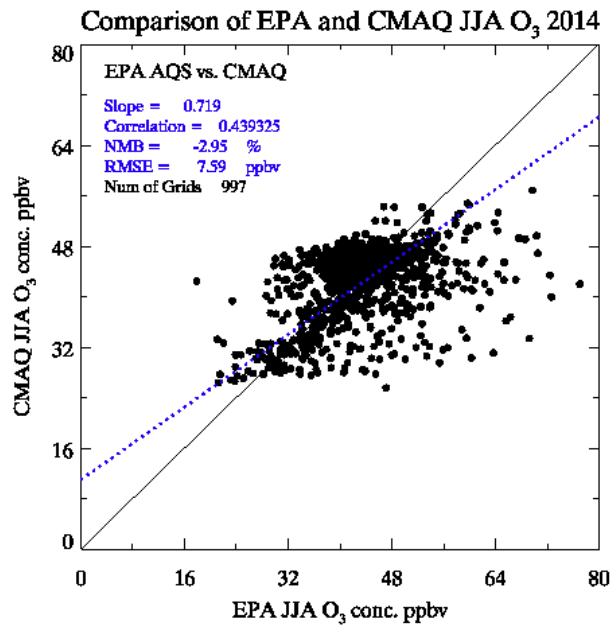
724

725 **Figure 5.** Comparison of summer MDA8 ozone concentrations from EPA AQS observations and  
 726 CMAQ simulations in 2014. AQS station data were gridded to the CMAQ grid using the EPA  
 727 RSIG software. a) Contour plot, the background stands for the CMAQ outputs and the dots stand  
 728 for gridded AQS observations; b) Scatter plot of the gridded AQS observations and co-located  
 729 CMAQ outputs.

730 a)

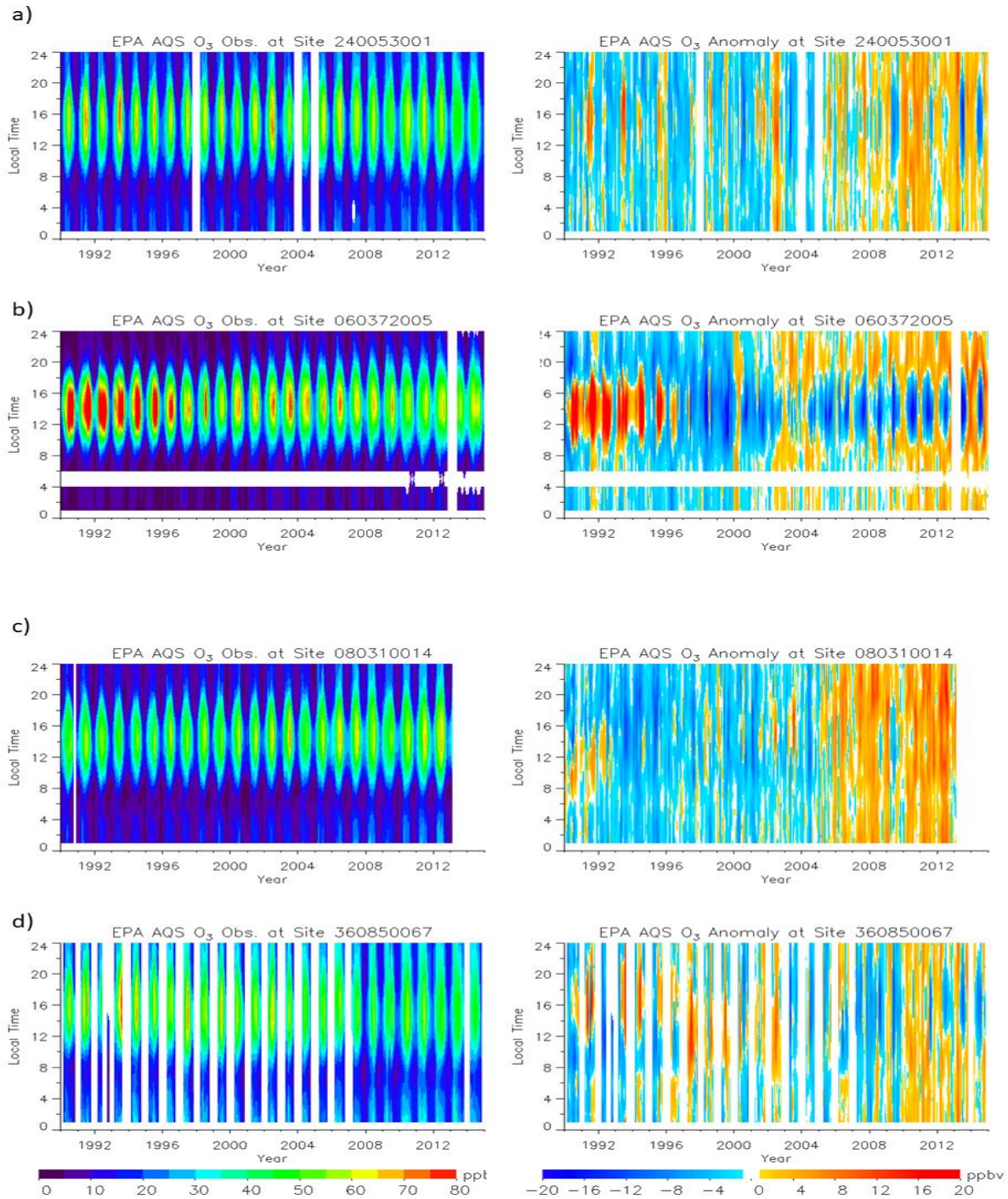


731  
 732 b)



733

734 **Figure 6.** The box-averaging analyses of AQS ozone observations at selected sites from 1990-  
 735 2015. a) Essex, Maryland (suburban Baltimore, AQS ID 240053001); b) Pasadena, California  
 736 (downtown Los Angeles, AQS ID 060372005); c) Denver, Colorado (downtown Denver, AQS ID  
 737 080310014); d) Staten Island, New York (suburban New York City, AQS ID: 360850067). Left  
 738 column shows the monthly mean, right column shows the anomaly values. White patches stand  
 739 for missing data or not sufficient data for the box-averaging analysis.

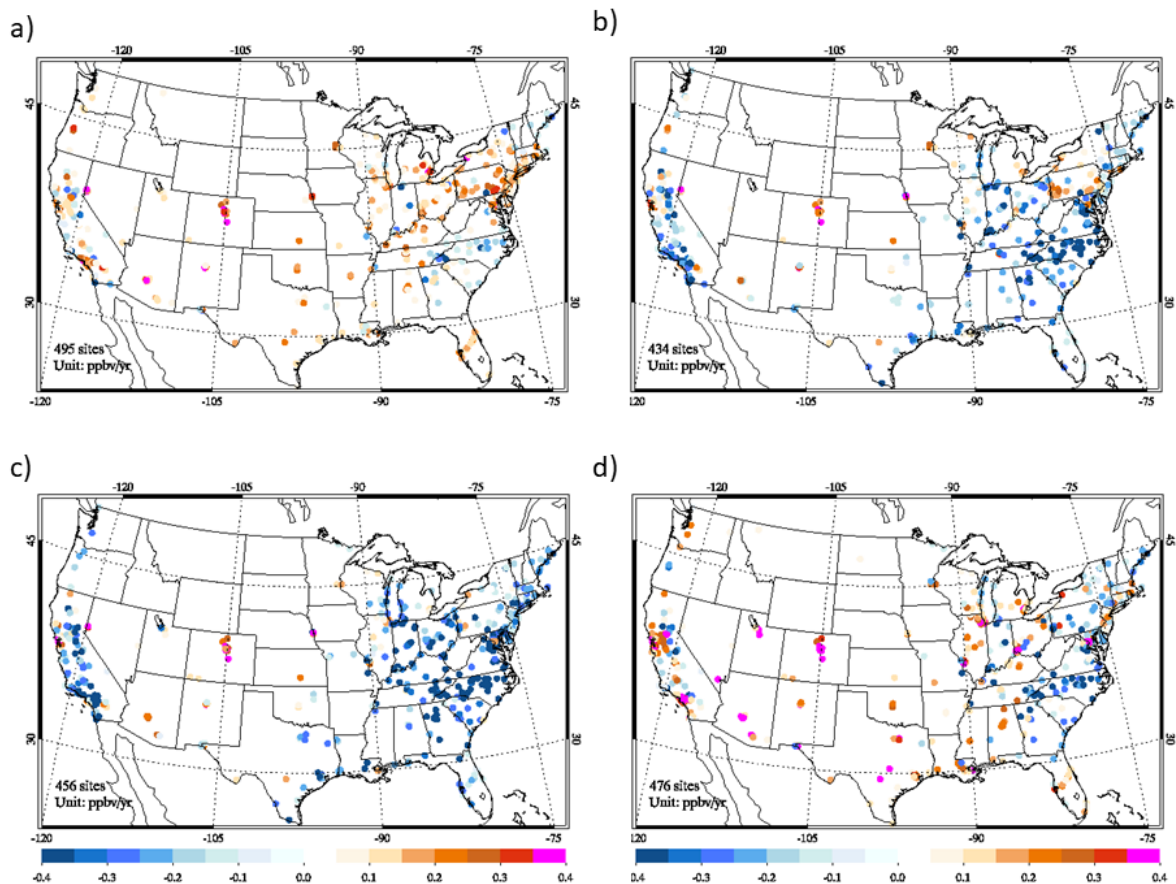


740

741

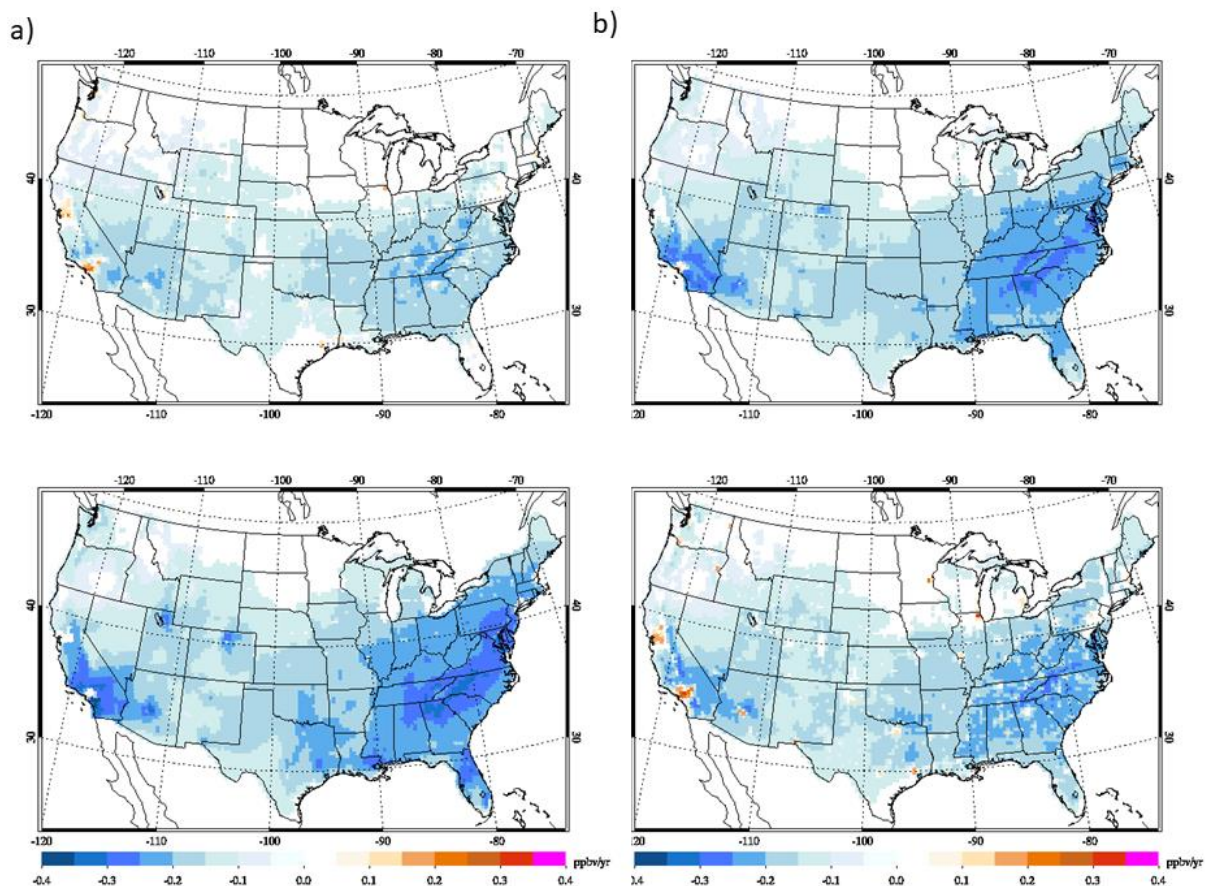


742 **Figure 7.** Trend in ozone observations at selected EPA AQS sites during 1990-2015 (Unit:  
743 ppbv/yr). a) at 8 am; b) at 12 pm; c) at 4 pm; d) at 8 pm (all local time). We only show the sites  
744 with statistically significant linear trend in the plots.



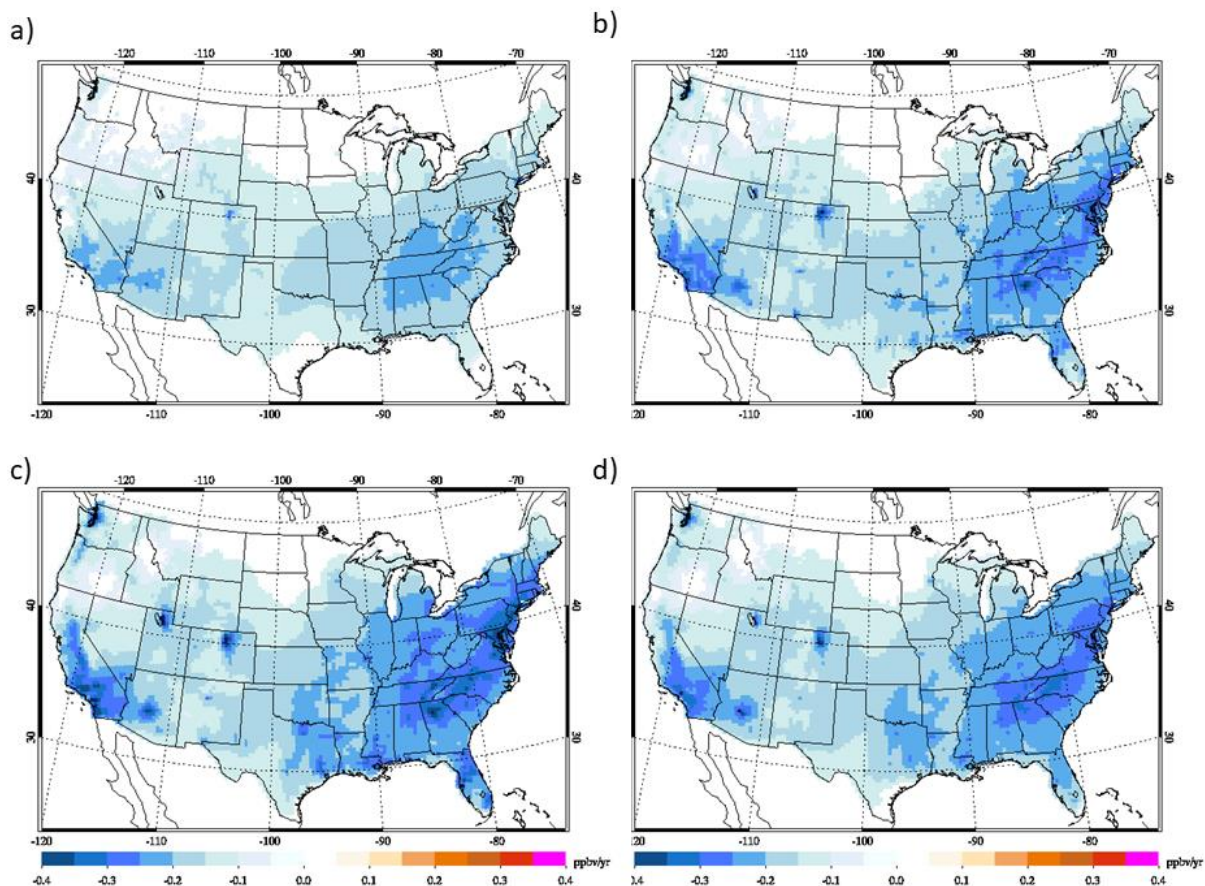
745

746 **Figure 8.** Trends in ozone simulations from CMAQ during 1990-2015 (Unit: ppbv/yr). a) at 8  
747 am; b) at 12 pm; c) at 4 pm; d) at 8 pm (all local time). We only show CMAQ grids with  
748 statistically significant linear trend in the plots.



749

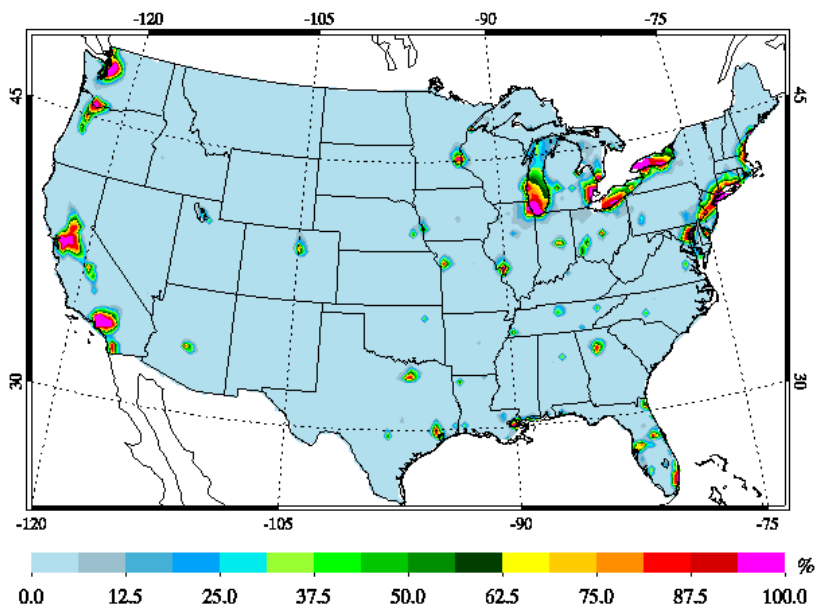
750 | **Figure 9.** Trend in  $O_x$  ( $O_x = O_3 + NO_2$ ) simulated by CMAQ during 1990-2015. a) at 8 am; b) at  
751 12 am; c) at 4 pm; d) at 8 pm (all local time). We only show CMAQ grids with statistically  
752 significant linear trend in the plots.



753

754 **Figure 10.** Probability of VOC-sensitive photochemical ozone production (i.e.,  $O_3/NO_y < 15$ ) in  
755 the CONUS simulated by CMAQ at 2 pm local time in July, a) 1995; b) 2005; and c) 2015

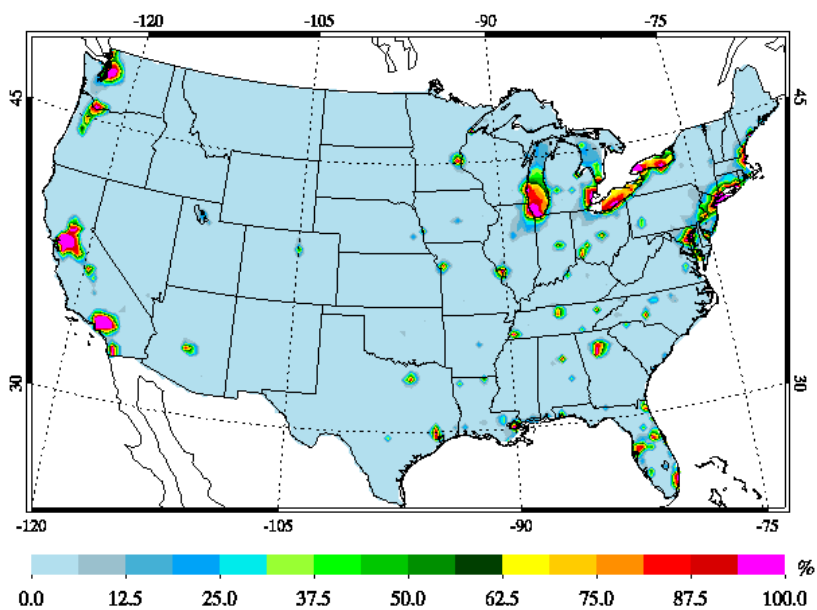
756 a)



757

758

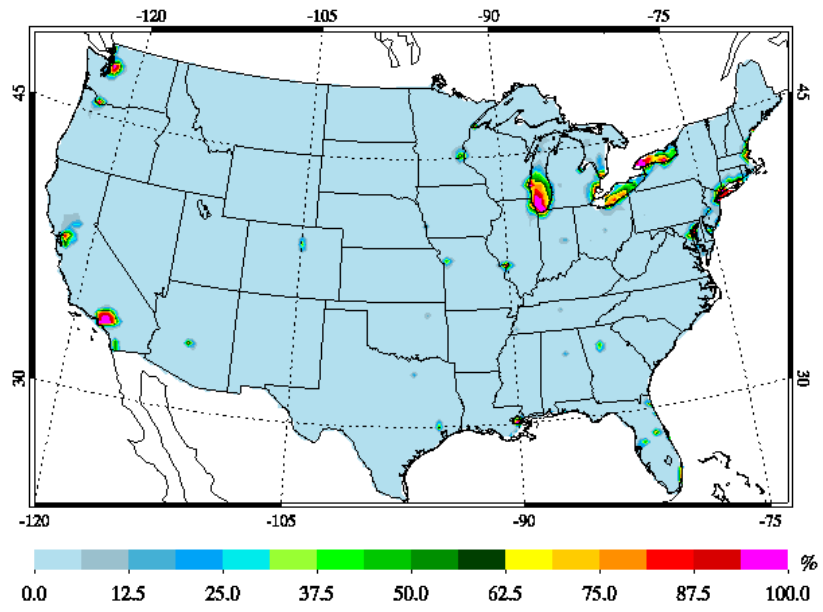
759 b)



760

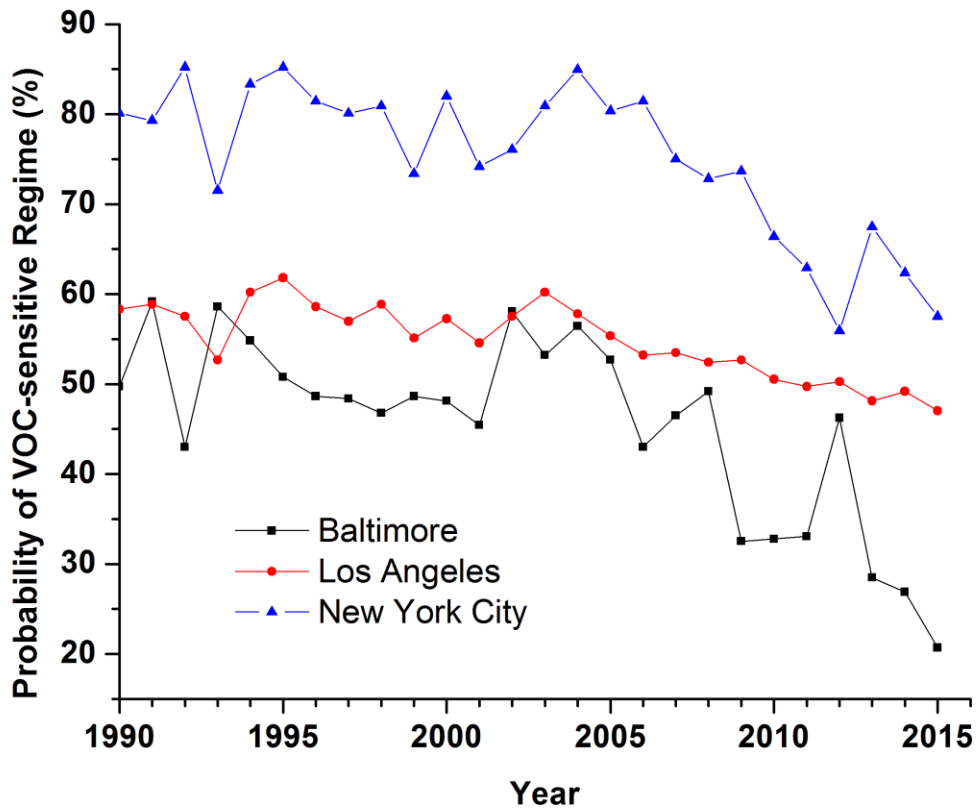
761

762 c)



763

764 **Figure 11.** Long-term trends in probability of VOC-sensitive photochemical production of  
765 surface ozone in three major urban areas at 2 pm in July. Probability is calculated using averages  
766 of  $3 \times 3$  grids centered at downtown.



767